J.L. Gonzalo Gomez, C. Bombardelli
Optimal Constant-Thrust Radius Change in Circular Orbit
Journal of Guidance Control and Dynamics, Vol. 42, N. 8, 2019, p. 1693-1708
doi:10.2514/1.G003134

Optimal Constant-Thrust Radius Change in Circular Orbit

Juan L. Gonzalo[1]
Politecnico di Milano, Milan 20156, Italy

Claudio Bombardelli[2]
Technical University of Madrid-UPM, 28040 Madrid, Spain

The problem of minimum-time, constant-thrust orbital transfer between coplanar circular orbits is revisited using a relative motion approach in curvilinear coordinates for the dynamics and an indirect optimization method. This is a continuation of a previous work where the authors studied the orbit rephasing problem. A linearization of state and costate equations leads to approximate analytical relations characterizing the evolution of the system dynamics and the optimal thrust profile as a function of a fundamental non-dimensional parameter, χ, which characterizes the maneuver duration. This approach allows one to study the range from very short to multi-revolution maneuvers using a unified framework. The optimal solution is seen to undergo a structural change as χ increases moving from a short to a long-maneuver regime and passing through a transition zone. Approximate expressions are obtained that can predict the maneuver duration with reasonable accuracy when sufficiently far from the transition zone. The full nonlinear problem characterized by an additional non-dimensional parameter is studied numerically, showing that the effect of nonlinearities can be accommodated by adopting a specific intermediate orbit as a reference. Examples of applications to Earth orbit, interplanetary missions and orbit control around small bodies are presented.

---

[1] Postdoctoral Research Fellow, Department of Aerospace Science and Technology, via Giuseppe La Masa 34; juanluis.gonzalo@polimi.it. Member AIAA
[2] Associate Professor, Space Dynamics Group, School of Aerospace Engineering (ETSIAE),Technical University of Madrid-UPM.

I. Introduction

The determination of the optimum control law to change the radius of a circular orbit in minimum time is a fundamental problem in astrodynamics and has been dealt with extensively in the past. One of the main contributions is the 1961 milestone paper of Theodore N. Edelbaum [1], which contains an approximate analytical solution for the optimum low thrust transfer between circular orbits including an inclination change maneuver. Edelbaum's solution applies very well to optimization cases where the transfer maneuver takes more than one revolution to be completed. The opposite condition, when the transfer takes less than a full revolution around the primary, has been investigated in other works (see, in particular, [2–4]). Among the previous references, the work by R. Broucke is especially significant as he provides an analytical solution (as a function of three parameters to be numerically determined) of the costate equations of the linearized problem in polar coordinates, finally leading to a generalization of the classical linear-tangent steering law. Other aspects of the problem have been investigated by different authors. Alfano and Thorne performed in [5] an extensive numerical optimization campaign to study the relation between the magnitude of the available thrust acceleration and the achievable velocity change. Casalino [6] investigated the limitations of Edelbaum's solution and proposed an approximate analytical method to extend Edelbaum's solution to the short-maneuver regime.

In this work, the minimum-time transfer between two coplanar, circular orbits is studied in depth using a new formulation for the system dynamics and exploiting linearization as a key element to construct approximate analytical solutions for the transfer time and thrust profile. It is a continuation of a previous work by the same authors [7], where the minimum-time, same-orbit rephasing problem was dealt with. Following the same approach, a nonlinear formulation in curvilinear coordinates is used to describe relative dynamics [8], and the optimal control problem in the thrust orientation is posed using the indirect method. While the focus is set to low-thrust transfers, a wide rage for the thrust parameter is considered. The formulation used for the relative motion differs from the classical solution by Clohessy and Wiltshire [9] in two aspects. On the one hand,

it introduces curvilinear coordinates to achieve a better description of the natural orbit curvature. On the other hand, it takes into account nonlinear terms to improve accuracy when initial velocity and displacement conditions are not very small. Together with the previous paper on the rephasing problem [7], this work completes the study on the minimum-time constant-thrust control between circular orbits in curvilinear coordinates.

The structure of the paper is as follows. First, the problem is described in detail by providing all the relevant assumptions, characteristic magnitudes, coordinate systems and dynamical models. Particular attention is given to the equations of motion and the boundary conditions, both for the exact (nonlinear) and linearized models, as well as to the choice of a reference orbit for the relative motion. Next, the minimum-time transfer problem is posed by applying Pontryagin's Maximum Principle to derive the first order optimality conditions, which take the form of a two-point boundary value problem (TPBVP). A qualitative understanding of the problem is then sought for by linearizing the TPBVP and comparing the orders of magnitude of the different terms in the equations. This a common technique in the field of fluid mechanics, but it is rarely applied to orbital dynamics. This analysis predicts the existence of two different regimes with fundamental qualitative differences depending on the ratio between the desired displacement and the available thrust χ. Approximate expressions relating the time of flight with the displacement-thrust ratio are also obtained, showing that, similarly to the optimum same-orbit rephasing problem (see [7]), the key difference between both regimes is whether the transfer takes less or more than one revolution of the reference orbit to complete (short- and long-maneuver regimes, respectively). Further developments allow one to find approximate analytical solutions for the linearized TPBVP fulfilling the boundary conditions, both for the short- and long-maneuver regimes, and to accommodate nonlinear effects by a judicious choice of the reference orbit. Finally, an extensive set of Earth-bound and interplanetary test cases is solved numerically using a multiple-shooting algorithm, both for the linearized and exact (nonlinear) models. The results confirm the qualitative findings of the analytical study, and allow one to evaluate the influence of the nonlinear effects. Several practical application examples are also provided to ease the physical interpretation of the results.

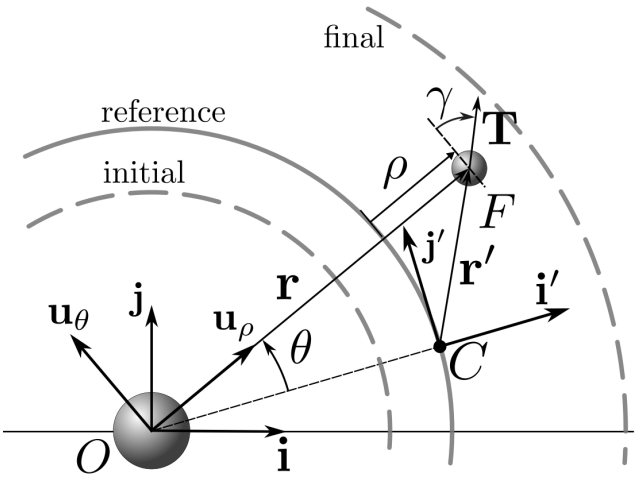

Fig. 1 Schematic representation of the problem. Compared to the rephasing problem in [7] there are now three orbits involved.

II. Problem Statement and Equations of Motion

This work studies the minimum-time transfer of a spacecraft subjected to constant thrust acceleration between two coplanar, circular orbits. The propellant mass expelled from the spacecraft m_{prop} is assumed to be negligible compared to its total mass m, so it can be taken as constant. As a consequence, this optimal control problem (OCP) would be equivalent to minimizing the total impulse required for the transfer.

A nonlinear relative motion formulation in curvilinear coordinates will be used for the dynamics [7, 8, 10]. Let us consider a chief C (either a real or 'virtual' object) describing a circular Keplerian orbit of radius R around a primary O with gravitational constant μ. From now on, all equations and variables will be expressed in nondimensional form taking the chief orbit radius R and inverse mean motion $\Omega^{-1} = \sqrt{R^3/\mu}$ as units of length and time, respectively. Let us also introduce an inertial reference frame $\mathcal{I} = \{O; \mathbf{i}, \mathbf{j}, \mathbf{k}\}$ and a local-vertical/local-horizontal one $\mathcal{C} = \{C; \mathbf{i}', \mathbf{j}', \mathbf{k}'\}$, as shown in Figure 1. The relative motion of a follower F (also real or virtual) with respect to the chief can then be expressed through two curvilinear coordinates ρ (follower radial separation from chief orbit) and θ (angle formed by the position vectors of follower and chief) associated to a cylindrical reference frame $\mathcal{F} = \{O; \mathbf{u}_\rho, \mathbf{u}_\theta, \mathbf{k}'\}$, where $\mathbf{u}_\rho$ and $\mathbf{u}_\theta$ are the radial and transversal unitary vectors for F, respectively. Note that it is straightforward to convert between (ρ, θ), the inertial position $\mathbf{r}$

and the relative position $\mathbf{r}'$ using geometrical relations (see [8]). Projecting the equations of relative motion onto $\mathcal{F}$ leads to [8]:

$$\begin{aligned} \ddot{\rho} - 2\dot{\theta} - 3\rho &= a_{i\rho} + a_{g\rho} + a_{\rho}^{T} \\ \ddot{\theta} + 2\dot{\rho} &= a_{i\theta} + \frac{a_{\theta}^{T}}{1+\rho} \end{aligned} \tag{1}$$

where ' $\cdot$ ' denotes the derivative with respect to the nondimensional time τ. Terms $a_{i\rho}$, $a_{g\rho}$, and $a_{i\theta}$ account for the nonlinear perturbing accelerations, which can be written as follows [7, 8]:

$$a_{i\rho} = \dot{\theta}^2 (1+\rho) + 2\dot{\theta}\rho\,, \quad a_{i\theta} = \frac{2\dot{\rho}\left(\rho - \dot{\theta}\right)}{1+\rho}\,,$$

$$a_{g\rho} = -2\rho + 1 - \frac{1}{(1+\rho)^2}\,,$$

whereas a_{ρ}^{T}, a_{θ}^{T} are the components in $\mathcal{F}$ of the thrust acceleration:

$$\left[\begin{array}{cc} a_{\rho}^{T} & a_{\theta}^{T} \end{array}\right] = \varepsilon \left[\begin{array}{cc} u_{\rho} & u_{\theta} \end{array}\right] = \varepsilon \mathbf{u}\,.$$

where ε is the nondimensional thrust acceleration, and $\mathbf{u}$ is the unitary thrust orientation vector. The thrust orientation angle γ (see Figure 1) can be defined as

$$\tan\gamma = \frac{u_{\rho}}{u_{\theta}}\,.$$

Given that ε is a constant parameter, $\mathbf{u}$ also represents the control vector for the problem.

It is convenient to express Eq. (1) as a first order system

$$\frac{\mathrm{d}\mathbf{S}}{\mathrm{d}\tau} = \mathbf{F}\left(\mathbf{S}, \mathbf{u}, \varepsilon; \tau\right)\,, \tag{2}$$

where $\mathbf{S}$ is a state vector defined as follows:

$$\mathbf{S} = \left[\begin{array}{cccc} \dot{\rho} & \dot{\theta} & \rho & \theta \end{array}\right]^{\top}\,, \tag{3}$$

and $\mathbf{F}$ is the right-hand side of the equations:

$$\mathbf{F}\left(\mathbf{S}, \mathbf{u}, \varepsilon; \tau\right) = \left[\begin{array}{c} 2\dot{\theta} + 3\rho + a_{i\rho} + a_{g\rho} + a_{\rho}^{T} \\ -2\dot{\rho} + a_{i\theta} + a_{\theta}^{T}/\left(1+\rho\right) \\ \dot{\rho} \\ \dot{\theta} \end{array}\right]\,. \tag{4}$$

By neglecting the nonlinear perturbing terms and assuming $\rho \ll 1$, a linear formulation with the same structure as the well-known Clohessy-Wiltshire equations is reached. The right-hand side of Eq. (2) for the linear formulation, denoted as $\mathbf{F}^*$ for clarity, can be written as follows:

$$\mathbf{F}^*\left(\mathbf{S}, \mathbf{u}, \varepsilon; \tau\right) \approx \begin{bmatrix} 2\dot{\theta} + 3\rho + a_\rho^T \\ -2\dot{\rho} + a_\theta^T \\ \dot{\rho} \\ \dot{\theta} \end{bmatrix}. \tag{5}$$

The initial and final states for the maneuver depend on the choice for departure, arrival and reference (chief) orbit. In all cases, the circular to circular orbit condition implies that the radial velocity will be zero, and the derivative of θ will be the difference between the mean motions of the current and reference orbits. In mathematical form:

$$\begin{aligned} \mathbf{S}\left(\tau_0\right) &= \begin{bmatrix} \dot{\rho}_0 & \dot{\theta}_0 & \rho_0 & \theta_0 \end{bmatrix}^\top = \begin{bmatrix} 0 & \sqrt{1/(1+\rho_0)^3} - 1 & \rho_0 & \theta_0 \end{bmatrix}^\top, \\ \mathbf{S}\left(\tau_f\right) &= \begin{bmatrix} \dot{\rho}_f & \dot{\theta}_f & \rho_f & \theta_f \end{bmatrix}^\top = \begin{bmatrix} 0 & \sqrt{1/(1+\rho_f)^3} - 1 & \rho_f & \theta_f \end{bmatrix}^\top, \end{aligned} \tag{6}$$

where subscripts 0 and f denote initial and final orbit, respectively. The desired radial displacement is $\Delta\rho = \rho_f - \rho_0$, the angular displacement is $\Delta\theta = \theta_f - \theta_0$, and the time of flight is $\Delta\tau = \tau_f - \tau_0$. Keep in mind that both $\Delta\rho$ and $\Delta\tau$ are non-dimensional magnitudes expressed in terms of the radius and inverse mean motion of the reference orbit. When the linearized equations of motion are used the boundary conditions should also be expressed in linear form, leading to:

$$\begin{aligned} \mathbf{S}^*\left(\tau_0\right) &= \begin{bmatrix} 0 & -3/2\rho_0 & \rho_0 & \theta_0 \end{bmatrix}^\top, \\ \mathbf{S}^*\left(\tau_f\right) &= \begin{bmatrix} 0 & -3/2\rho_f & \rho_f & \theta_f \end{bmatrix}^\top. \end{aligned} \tag{7}$$

From now on $\Delta\theta$ will be set free, implying that the phasing problem will be solved by simply selecting the phasing at which the maneuver is started. This is a fuel-efficient solution for LEO orbits, separating it from the radius modification problem. Moreover, it is possible to further simplify the problem by setting $\theta_0 = 0$ and $\tau_0 = 0$, leading to $\theta_f = \Delta\theta$ and $\tau_f = \Delta\tau$. Regarding the choice of reference orbit, two particular cases will be considered henceforth: reference orbit coincident with either the initial or final orbit. They correspond, respectively, to $\rho_0 = 0$, $\rho_f = \Delta\rho$ and $\rho_0 = -\Delta\rho$, $\rho_f = 0$.

III. Maneuver Optimization

The cost function for the minimum-time constant-thrust transfer between two coplanar, circular orbits can be expressed in the form[11]:

$$J = \int_0^{\Delta\tau} L\left(\mathbf{S}, \mathbf{u}; \tau\right) \mathrm{d}\tau \, = \Delta\tau \, ,$$

where $L = 1$ is the Lagrangian. Since the cost function does not depend on the final state, this is a particular case of a Problem of Lagrange. From this objective function a Hamiltonian is defined as:

$$H\left(\mathbf{S}, \boldsymbol{\lambda}, \mathbf{u}; \tau\right) = \boldsymbol{\lambda}^{\top} \mathbf{F} + L \tag{8}$$

where

$$\boldsymbol{\lambda} = \left[\begin{array}{cccc} \lambda_u & \lambda_v & \lambda_\rho & \lambda_\theta \end{array} \right]^{\top} , \tag{9}$$

is the costate associated to the state $\mathbf{S}$. The equations of motion can then be written in the following form:

$$\dot{\mathbf{S}} = \frac{\partial H}{\partial \boldsymbol{\lambda}} \, , \tag{10}$$

and the evolution of the costate is given by the adjoint (or costate) equations derived from the first order optimality conditions[11]:

$$\dot{\boldsymbol{\lambda}} = -\frac{\partial H}{\partial \mathbf{S}} \, . \tag{11}$$

An expression for $\mathbf{u}\left(\mathbf{S}, \boldsymbol{\lambda}; \tau\right)$ is now sought for using the Pontryagin Maximum (or minimum) Principle[12], which states that the optimal control for a given optimal trajectory is the one that leads to an extreme value of H over the set of admissible controls. Mathematically (for the minimization case):

$$\mathbf{u}^{-}\left(\tau\right) = \underset{\mathbf{u} \in \mathbf{U}}{\arg\min} \, H\left(\mathbf{S}^{-}\left(\tau\right), \boldsymbol{\lambda}^{-}\left(\tau\right), \mathbf{u}; \tau\right) \quad \forall \tau \in \left[0, \Delta\tau\right] \, ,$$

where the superscript '$-$' denotes the optimal trajectory and $\mathbf{U}$ is the set of valid controls, which in this case corresponds to:

$$\mathbf{U} = \left\{ \mathbf{u} \in \mathbb{R}^2 / ||\mathbf{u}|| = 1 \right\} \, ,$$

that is, $\mathbf{u}$ must be a unitary vector. Gathering the terms in H involving the control vector one reaches:

$$\varepsilon u_\rho \lambda_u + \varepsilon \frac{u_\theta}{1+\rho}\lambda_v = \varepsilon \begin{bmatrix} \lambda_u & \frac{\lambda_v}{1+\rho} \end{bmatrix} \cdot \mathbf{u}$$

It follows that, for this contribution to minimize H for all τ, the vectors in the previous expression must have opposite directions. Together with the unitary requirement for $\mathbf{u}$ this leads to:

$$u_\rho = -\frac{\lambda_u}{\sqrt{\lambda_u^2 + \left(\frac{\lambda_v}{1+\rho}\right)^2}}, \quad u_\theta = -\frac{\frac{\lambda_v}{1+\rho}}{\sqrt{\lambda_u^2 + \left(\frac{\lambda_v}{1+\rho}\right)^2}}. \tag{12}$$

Interestingly, for the linear case this expression reduces to $\mathbf{u} = [\lambda_u \, \lambda_v]$, which has the same expression as the primer vector in cartesian coordinates[13, 14].

Substituting Eq. (12) into Eq. (11) and operating one reaches:

$$\begin{aligned}
\dot{\lambda}_u &= -\frac{\partial H}{\partial \dot{\rho}} = 2\lambda_v \frac{1+\dot{\theta}}{1+\rho} - \lambda_\rho \\
\dot{\lambda}_v &= -\frac{\partial H}{\partial \dot{\theta}} = -2\lambda_u (1+\rho)(1+\dot{\theta}) + \lambda_v \frac{2\dot{\rho}}{1+\rho} - \lambda_\theta \\
\dot{\lambda}_\rho &= -\frac{\partial H}{\partial \rho} = -\lambda_u \left[\left(1+\dot{\theta}\right)^2 + \frac{2}{(1+\rho)^3} \right] - \lambda_v \frac{2\dot{\rho}\left(1+\dot{\theta}\right) + \varepsilon\left(-2u_\theta + u_\theta^3\right)}{(1+\rho)^2} \\
\dot{\lambda}_\theta &= -\frac{\partial H}{\partial \theta} = 0 .
\end{aligned} \tag{13}$$

The last equation indicates that the costate associated to the angular coordinate is constant. Moreover, given that at least one of the boundary values (BVs) for θ is free the corresponding costate will be zero.

One last optimality condition is needed to account for the free final time. Imposing J to be stationary with respect to variations in $\Delta\tau$ leads to the following transversality condition[11]:

$$H(\Delta\tau) = 0 . \tag{14}$$

Substituting the known values of the final state and recalling that λ_θ is zero for all τ, Eq. (14) takes a simpler form:

$$\lambda_u(\Delta\tau)^2 + \left[\frac{\lambda_v(\Delta\tau)}{1+\rho_f}\right]^2 = \frac{1}{\varepsilon^2} . \tag{15}$$

Equations (2), (13) and (15) form a differential-algebraic system of eight Ordinary Differential Equations (state and costate equations) and one algebraic equation (transversality condition). The

state boundary conditions are given by Eq. (6), where the values of ρ_0 and ρ_f depend on the choice for the reference orbit. All the state BVs are fixed except for the total angular displacement, implying that the corresponding costate BVs will be unknown parameters except for the final λ_θ which will be zero:

$$\begin{aligned} \boldsymbol{\lambda}(0) &= \begin{bmatrix} \lambda_{u0} & \lambda_{v0} & \lambda_{\rho 0} & \lambda_{\theta 0} \end{bmatrix}^\top , \\ \boldsymbol{\lambda}(\Delta\tau) &= \begin{bmatrix} \lambda_{uf} & \lambda_{vf} & \lambda_{\rho f} & 0 \end{bmatrix}^\top . \end{aligned} \tag{16}$$

Gathering these results, the OCP now takes the form of a TPBVP with 8 differential equations describing the time evolution of state and costate, 9 terminal constraints (7 fixed state BVs, 1 fixed costate BV, and the transversality condition), and 9 unknowns (7 unknown costate BVs, the angular displacement and the time of flight). However, it was already noted that according to the last of Eq. (13) λ_θ is constant, so $\lambda_{\theta 0} = \lambda_\theta(\Delta\tau) = 0$ and the TPBVP dimension can be reduced to 8. Moreover, none of the equations depends explicitly on θ, so it is possible to take $\Delta\theta$ and the corresponding equation out of the TPBVP further reducing its dimension to 7.

The full TPBVP cannot be solved analytically for a general case. In the remainder of this section the problem will be studied from a qualitative point of view, with the aim of extracting knowledge about the structure of the solution and the evolution of the state. This information can then be used to generate initial guesses for the iterative numerical method presented in the next section. To ease the treatment of the equations, the linearized formulation of the relative motion in curvilinear coordinates, Eq. (5), is used, yielding the Hamiltonian:

$$H^* = \boldsymbol{\lambda}^\top \mathbf{F}^* = \lambda_u \left(2\dot{\theta} + 3\rho + \varepsilon u_\rho\right) + \lambda_v \left(-2\dot{\rho} + \varepsilon u_\theta\right) + \lambda_\rho \dot{\rho} + \lambda_\theta \dot{\theta} + 1 \, .$$

This leads to the following set of adjoint equations:

$$\begin{aligned} \dot{\lambda}_{\dot{\rho}} &= -\frac{\partial H^*}{\partial \dot{\rho}} = -\lambda_\rho + 2\lambda_v \\ \dot{\lambda}_{\dot{\theta}} &= -\frac{\partial H^*}{\partial \dot{\theta}} = -2\lambda_u - \lambda_\theta \\ \dot{\lambda}_\rho &= -\frac{\partial H^*}{\partial \rho} = -3\lambda_u \\ \dot{\lambda}_\theta &= -\frac{\partial H^*}{\partial \theta} = 0 \end{aligned} \tag{17}$$

Note that, by neglecting the nonlinear terms in the dynamics, the adjoint equations have been decoupled from the equations of motion. Their solution along with the boundary conditions in

Eq. (16) is now straightforward

$$\lambda_u = A\sin(\tau+\varphi)$$

$$\lambda_v = 2A\cos(\tau+\varphi)+C$$

$$\lambda_\rho = 3A\cos(\tau+\varphi)+2C$$

$$\lambda_\theta = 0$$

where the three parameters A, C, and φ are related to the initial value of the costate as follows:

$$\lambda_{u0} = A\sin\varphi\,, \quad \lambda_{v0} = 2A\cos\varphi + C\,, \quad \lambda_{\rho 0} = 3A\cos\varphi + 2C\,,$$

$$A = \sqrt{\lambda_{u0}^2 + (2\lambda_{v0}-\lambda_{\rho 0})^2}\,, \quad C = 2\lambda_{\rho 0} - 3\lambda_{v0}\,, \quad \varphi = \mathrm{atan2}\left(\lambda_{u0}, 2\lambda_{v0}-\lambda_{\rho 0}\right)\,.$$

A further simplification can be achieved by exploiting the symmetry properties of the linearized problem (see Pontani[15]) to express φ as a function of the time of flight, thus removing one unknown from the TPBVP. First of all, note that λ_u and λ_v have opposite behaviors regarding symmetry, one of them will be odd and the other even. However, λ_v cannot be odd for $C \neq 0$, leading to λ_u odd and λ_v even. The symmetry conditions then yield:

$$\sin(\Delta\tau/2+\varphi) = 0\,, \quad \cos(\Delta\tau/2+\varphi) = \pm 1\,,$$

which yields:

$$\varphi = -\Delta\tau/2 + n\pi\,, \quad n \in \mathbb{N}^0\,,$$

where the value of n determines whether the cosine has a maximum (n even) or a minimum (n odd) at $\tau = \Delta\tau/2$. Given that the value of n only changes the sign of the trigonometric functions and they are always multiplied by A, it is possible to arbitrarily set $n = 0$ and let the sign be determined by A. The costate equations for the linearized problem then reduce to:

$$\begin{aligned}
\lambda_u &= A\sin(\tau-\Delta\tau/2) \\
\lambda_v &= 2A\cos(\tau-\Delta\tau/2)+C \\
\lambda_\rho &= 3A\cos(\tau-\Delta\tau/2)+2C \\
\lambda_\theta &= 0
\end{aligned} \tag{18}$$

There is no closed form solution for the linearized equations of motion perturbed by a thrust acceleration, so it is not possible to find a fully analytical solution for the OCP even in the linearized case. Nevertheless, additional information on the solution can be obtained by analyzing the orders of magnitude of the different terms in the equations and locating the dominant ones, following a procedure similar to [7]. To this end, a new non-dimensionalization is introduced taking $\Delta r = |\Delta\rho|$ and $\Delta\tau$ as characteristic displacement and time respectively:

$$\frac{\mathrm{d}^2\hat{\rho}}{\mathrm{d}\hat{\tau}^2} = 2\Delta\tau\frac{\mathrm{d}\hat{\theta}}{\mathrm{d}\hat{\tau}} + 3\Delta\tau^2\hat{\rho} + Ku_\rho\,, \tag{19}$$

$$\frac{\mathrm{d}^2\hat{\theta}}{\mathrm{d}\hat{\tau}^2} = -2\Delta\tau\frac{\mathrm{d}\hat{\rho}}{\mathrm{d}\hat{\tau}} + Ku_\theta\,, \tag{20}$$

with:

$$\hat{\tau} = \frac{\tau}{|\Delta\tau|}\,, \quad \hat{\rho} = \frac{\rho}{\Delta r}\,, \quad \hat{\theta} = \frac{\theta}{\Delta r}\,, \quad K = \frac{\Delta\tau^2}{\chi}\,,$$

where:

$$\chi = \frac{\Delta r}{\varepsilon}\,,$$

is the non-dimensional ratio between the desired displacement and the available thrust acceleration. The boundary conditions now take the form:

$$\begin{aligned}\hat{\mathbf{S}}(0) &= \begin{bmatrix} 0 & \hat{\theta}_0' & \hat{\rho}_0 & \hat{\theta}_0 \end{bmatrix}^\top = \begin{bmatrix} 0 & -3/2\Delta\tau\hat{\rho}_0 & \hat{\rho}_0 & 0 \end{bmatrix}^\top\,,\\ \hat{\mathbf{S}}(1) &= \begin{bmatrix} 0 & \hat{\theta}_f' & \hat{\rho}_f & \hat{\theta}_f \end{bmatrix}^\top = \begin{bmatrix} 0 & -3/2\Delta\tau\hat{\rho}_f & \hat{\rho}_f & \Delta\theta/\Delta r \end{bmatrix}^\top\,.\end{aligned} \tag{21}$$

Introducing the symbols

$$\pm_\Delta = \mathrm{sign}\,(\Delta\rho)\,, \quad \mp_\Delta = -\mathrm{sign}\,(\Delta\rho)\,,$$

the radial boundary values for the case where the initial orbit is taken as reference are:

$$\hat{\rho}_0 = 0\,, \quad \hat{\rho}_f = \pm_\Delta 1\,,$$

whereas if the final orbit is used as reference they can be written as:

$$\hat{\rho}_0 = \mp_\Delta 1\,, \quad \hat{\rho}_f = 0\,,$$

being in all cases $\Delta\hat{\rho} = \hat{\rho}_f - \hat{\rho}_0 = \pm_\Delta 1$.

The orders of magnitude for each term in Eqs. (19,20) are:

$$\frac{\mathrm{d}^2\hat{\rho}}{\mathrm{d}\hat{\tau}^2} \sim 1\,, \quad \Delta\tau\frac{\mathrm{d}\hat{\theta}}{\mathrm{d}\hat{\tau}} \sim \Delta\tau\frac{\Delta\theta}{\Delta r}\,, \quad \Delta\tau^2\hat{\rho} \sim \Delta\tau^2\,, \quad Ku_\rho \sim \frac{\Delta\tau^2}{\chi}u_\rho\,,$$

$$\frac{\mathrm{d}^2\hat{\theta}}{\mathrm{d}\hat{\tau}^2} \sim \frac{\Delta\theta}{\Delta r}\,, \quad \Delta\tau\frac{\mathrm{d}\hat{\rho}}{\mathrm{d}\hat{\tau}} \sim \Delta\tau\,, \quad Ku_\theta \sim \frac{\Delta\tau^2}{\chi}u_\theta\,,$$

where:

$$u_\rho^2 + u_\theta^2 = 1\,, \quad |u_\rho|, |u_\theta| \leq 1\,.$$

According to Eq. (20), the angular displacement can be driven both by gravitational effects and the action of thrust. Making the hypothesis that the second is at least as important as the first, by comparing the transversal acceleration with the thrust component one reaches:

$$\frac{\Delta\theta}{\Delta r} \sim \frac{\Delta\tau^2}{\chi}u_\theta\,.$$

Introducing this into the orders of magnitude relations for Eq. (19) yields:

$$\frac{\mathrm{d}^2\hat{\rho}}{\mathrm{d}\hat{\tau}^2} \sim 1\,, \quad \Delta\tau\frac{\mathrm{d}\hat{\theta}}{\mathrm{d}\hat{\tau}} \sim \frac{\Delta\tau^3}{\chi}u_\theta\,, \quad \Delta\tau^2\hat{\rho} \sim \Delta\tau^2\,, \quad Ku_\rho \sim \frac{\Delta\tau^2}{\chi}u_\rho\,.$$

It is now possible to distinguish the limit cases for $\Delta\tau \gg 1$, long-maneuver regime, and $\Delta\tau \ll 1$, short-maneuver regime. For the long-maneuver regime ($\Delta\tau \gg 1$) the second and third terms of Eq. (19) are dominant, leading to:

$$\Delta\tau \sim \frac{\chi}{|u_\theta|}\,,$$

which not only gives a first estimate of the required maneuver time, but also shows that the optimum thrust orientation profile will remain as close as possible to the transversal direction (the need to fulfill all the boundary conditions will of course introduce deviations). For the short-maneuver regime ($\Delta\tau \ll 1$) the first and fourth terms of Eq. (19) become dominant (note that at least one control term must be retained), giving the following estimate for the maneuver time:

$$\Delta\tau \sim \sqrt{\frac{\chi}{|u_\rho|}}\,.$$

The preferred orientation of thrust for minimum time has now changed with respect to the long-maneuver regime, from the transversal to the radial direction.

These results have been obtained under the hypothesis that transversal thrust was at least as important as gravitational effects in their respective equation of motion. Therefore, before accepting them as valid we have to check whether this hypothesis holds. The following developments not only will prove this true, but also show that the Coriolis term is non-negligible too. In the long-maneuver regime, $\Delta\tau \gg 1$, introducing the estimation for $\Delta\tau$ into the orders of magnitude for Eq. (20) yields (note that ' $\prime$ ' denotes derivative with respect to $\hat{\tau}$):

$$\hat{\theta}'' \sim \frac{\Delta\theta}{\Delta r}\,, \quad \Delta\tau\hat{\rho}' \sim \Delta\tau\,, \quad Ku_\theta \sim \Delta\tau\,,$$

showing that both gravitational and thrust effects are of the same order, and giving an estimate for $\Delta\theta$:

$$\Delta\theta \sim \Delta\tau\Delta r\,.$$

Interestingly, Eq. (19) previously showed that the desired displacement in $\hat{\rho}$ was reached through the coupling between both equations due to the Coriolis term, so this regime is driven by gravitational effects. In the short-maneuver regime, $\Delta\tau \ll 1$, the orders of magnitude for Eq. (20) read:

$$\hat{\theta}'' \sim \frac{\Delta\theta}{\Delta r}\,, \quad \Delta\tau\hat{\rho}' \sim \Delta\tau\,, \quad Ku_\theta \sim \frac{u_\theta}{u_\rho}\,.$$

There are two opposing criteria regarding the magnitude of u_θ. On the one hand, u_θ should be as small as possible since the preferred thrust orientation for minimum time is radial. On the other hand, transversal control needs to be non-negligible in order to ensure the fulfillment of the boundary conditions in $\hat{\theta}'$. Therefore, the transversal acceleration term will be at most of the same order as the other two. Comparing the acceleration and Coriolis terms leads to the same $\Delta\theta$ estimate already obtained for the long-maneuver regime, $\Delta\theta \sim \Delta\tau\Delta r$, while comparing the acceleration and Coriolis terms yields $u_\theta \lesssim \Delta\tau \ll 1$ (that is, the shorter the maneuver time the closer the thrust profile will be to the radial direction). Since the displacement in $\hat{\rho}$ is mainly driven by the direct action of thrust in the radial direction, this regime is dominated by thrust effects.

The transition between both regimes takes place for

$$\Delta\tau \sim \mathcal{O}(1) \;\Rightarrow\; \Delta r \sim \varepsilon\,.$$

In this transition zone, all terms in both equations become of the same order, and no simplifications can be made. The structure of the solution undergoes fundamental qualitative changes as it moves from one regime to the other, transitioning from nearly radial thrust orientation for the short-maneuver regime to nearly tangential for the long-maneuver regime. Since $\Delta\tau = 2\pi$ corresponds to one orbital revolution of the leader, it follows that a key physical difference between both regimes is whether the maneuver requires only a small fraction of an orbital revolution to complete (short-maneuver regime) or several (long-maneuver regime).

For consistency and convenience, in further developments the linear costate solutions, Eq. (18), will also be expressed in non-dimensional form as follows:

$$\begin{aligned}
\hat{\lambda}_u &= \varepsilon\lambda_u = \hat{A}\sin\left(\Delta\tau\tilde{\tau}\right) \\
\hat{\lambda}_v &= \varepsilon\lambda_v = 2\hat{A}\cos\left(\Delta\tau\tilde{\tau}\right) + \hat{C} \\
\hat{\lambda}_\rho &= \varepsilon\lambda_\rho = 3\hat{A}\cos\left(\Delta\tau\tilde{\tau}\right) + 2\hat{C} \\
\hat{\lambda}_\theta &= \varepsilon\lambda_\theta = 0
\end{aligned} \tag{22}$$

with:

$$\hat{A} = \varepsilon A\,, \quad \hat{C} = \varepsilon C\,, \quad \tilde{\tau} = \hat{\tau} - 1/2\,,$$

where a change in the origin of the time variable has been introduced to better reflect the symmetry properties of the linearized solution.

A more accurate description for the short and long-maneuver regimes is obtained in the following subsections by solving the approximate problem resulting from neglecting the non-dominant terms in the linearized equations of motion. This kind of approximate analytical analysis cannot be carried out for the transition zone, where all the terms in the equations become of comparable order. In the absence of an approximate analytical solution, this transition zone will be studied numerically.

A. Short-maneuver regime

The previous results for the short-maneuver regime already show that $|u_\rho| \sim 1$, but it is possible to obtain additional information on the control using the costate solutions for the linearized problem.

Expanding the first two of Eq. (22) in Taylor series around $\tilde{\tau} = 0$ for $\Delta\tau \ll 1$ yields:

$$\begin{aligned} \hat{\lambda}_u &= \hat{A}\Delta\tau\tilde{\tau} + \mathcal{O}\left(\Delta\tau^3\right) , \\ \hat{\lambda}_v &= \hat{C} + 2\hat{A} - \hat{A}\Delta\tau^2\tilde{\tau}^2 + \mathcal{O}\left(\Delta\tau^4\right) , \end{aligned} \tag{23}$$

and the $|u_\rho| \gg |u_\theta|$ condition implies that:

$$\left|\hat{C} + 2\hat{A}\right| \ll \left|\hat{A}\Delta\tau\right| . \tag{24}$$

Introducing the expansions for the costate into the transversality condition, Eq. (15), and retaining only the leading order terms (taking into account the previous inequality) yields:

$$\hat{A} \approx \pm\frac{2}{\Delta\tau} .$$

Plugging this value into Eq. (24), an estimation for $\hat{C}$ is also obtained:

$$\hat{C} \approx -2\hat{A} \approx \mp\frac{4}{\Delta\tau} .$$

Gathering these results, the leading component of the primer vector can be approximated for $\Delta\tau \ll 1$ as:

$$\hat{\lambda}_u \approx \pm 2\tilde{\tau} .$$

This expression together with Eq. (12) show that the radial component of thrust has exactly one change of sign at the middle point of the maneuver. Since the control is known to be preferably aligned in the radial direction, this leads to a nearly bang-bang control.

Neglecting small terms in the linearized equations of motion, Eqs. (19,20), for the short-maneuver regime yields:

$$\hat{\rho}'' \approx K u_\rho , \tag{25}$$

$$\hat{\theta}'' + 2\Delta\tau\hat{\rho}' \approx K u_\theta . \tag{26}$$

Knowing that control is nearly bang-bang, it is straightforward to check from Eq. (25) that a positive $\Delta\rho$ requires thrust to be initially oriented along the positive radial direction (an vice versa). Along with Eq. (12), this allows to determine the correct signs for the costate:

$$\hat{\lambda}_u \approx \pm_\Delta 2\tilde{\tau} \approx \pm_\Delta \left(2\hat{\tau} - 1\right) ,$$

$$\hat{A} \approx \pm_\Delta \frac{2}{\Delta\tau}\,, \quad \hat{C} \approx \mp_\Delta \frac{4}{\Delta\tau}\,.$$

Assuming control is strictly bang-bang and taking the previous signs into account, Eq. (25) can be solved as:

$$\hat{\rho} - \hat{\rho}_0 \approx \pm_\Delta \begin{cases} K\dfrac{\hat{\tau}^2}{2} & 0 < \hat{\tau} < 1/2 \\ K\left(-\dfrac{\hat{\tau}^2}{2} + \hat{\tau} - \dfrac{1}{4}\right) & 1/2 < \hat{\tau} < 1 \end{cases}$$

An estimate for the time of flight can now be obtained by imposing the desired radial displacement $\Delta\hat{\rho} = \pm_\Delta 1$:

$$\Delta\tau \approx 2\sqrt{\chi}\,, \tag{27}$$

where all parameters involved are non-dimensional. This solution for $\hat{\rho}$ fulfills the boundary conditions in position and, due to the control symmetry, also in velocity. Building on this result, it would be possible to obtain an expression for $\hat{\theta}$ in the bang-bang control limit by taking $u_\theta = 0$ in Eq. (26) and integrating. However, said $\hat{\theta}$ would separate appreciably from the actual optimal maneuver, and particularly it could not fulfill the boundary conditions in velocity since it would take the same value at both extremes. The reason is that the transversal component of thrust, albeit small, can be of the same order as the other terms in the transversal equation and cannot be neglected.

The previous approximation was based on neglecting $\hat{C} + 2\hat{A}$ in the series expansion for the primer vector, supported by the knowledge that it must be preferably oriented along the radial direction. However, a closer look at Eq. (23) reveals that, since $\tilde{\tau}$ crosses 0, no matter how small that term is there will always be a region near the bang-bang switch where its contribution is dominant. In order to reach a better approximation fulfilling all the boundary conditions, this switching region must be preserved. To this end, a change of parameter is proposed for $\hat{C}$ based on Eq. (24):

$$\hat{C} + 2\hat{A} = c\hat{A}\Delta\tau^2\,. \tag{28}$$

The series expansion for $[\lambda_u\ \lambda_v]$ can now be written as:

$$\hat{\lambda}_u = \hat{A}\Delta\tau\tilde{\tau} - \frac{1}{6}\hat{A}\Delta\tau^3\tilde{\tau}^3 + \mathcal{O}\left(\Delta\tau^5\right)\,,$$

$$\hat{\lambda}_v = \hat{A}\Delta\tau^2\left(c - \tilde{\tau}^2\right) + \mathcal{O}\left(\Delta\tau^4\right)\,,$$

and the square of its norm:

$$\hat{\lambda}_u^2 + \hat{\lambda}_v^2 = \hat{A}^2 \Delta\tau^2 \left[c^2 \Delta\tau^2 + \left(1 - 2c\Delta\tau^2\right) \tilde{\tau}^2 + \frac{2}{3} \Delta\tau^2 \tilde{\tau}^4 \right] + \mathcal{O}\left(\Delta\tau^6\right) .$$

Because $\Delta\tau \ll 1$ and $|\tilde{\tau}| \leq 1/2$, the leading term of this norm will be the one in $\tilde{\tau}^2$ save for a small region around 0 where the constant part will dominate; it is straightforward to check that both contributions become equal for $\tilde{\tau}^2 = c^2\Delta\tau^2/(1 - 2c\Delta\tau^2)$. Neglecting the term in $\tilde{\tau}^4$ (whose contribution will always be smaller) and knowing from the previous solution that $\hat{A}/|\hat{A}| = \pm_\Delta 1$, it is possible to propose a new control vector in the form:

$$u_\rho \approx \mp_\Delta \frac{\tilde{\tau}}{\sqrt{c^2\Delta\tau^2 + \left(1 - 2c\Delta\tau^2\right)\tilde{\tau}^2}} ,$$

$$u_\theta \approx \mp_\Delta \frac{\Delta\tau \left(c - \tilde{\tau}^2\right)}{\sqrt{c^2\Delta\tau^2 + \left(1 - 2c\Delta\tau^2\right)\tilde{\tau}^2}} .$$

Eqs. (25,26) can be solved for this control vector and the initial conditions in Eq. (21), obtaining the radial solution first and then substituting into the transversal equation. The resulting $\hat{\rho}$ and $\hat{\theta}$ can be expressed in a compact way as:

$$\hat{\rho}' = \pm_\Delta K \frac{K_1 - g}{K_2} ,$$

$$\hat{\rho} - \hat{\rho}_0 = \pm_\Delta K \left[\frac{K_1 \left(1 + 4\tilde{\tau}\right) - 2g\tilde{\tau}}{4K_2} - \frac{c^2\Delta\tau^2}{2K_2^{3/2}} g_2 \right] ,$$

$$\hat{\theta}' - \hat{\theta}_0' = \pm_\Delta \Delta\tau K \left[\frac{-K_1 \left(1 + 8\tilde{\tau}\right) + 6g\tilde{\tau}}{4K_2} + \frac{c\left(-2 + 5c\Delta\tau^2\right)}{2K_2^{3/2}} g_2 \right] ,$$

$$\hat{\theta} - \hat{\theta}_0 = \hat{\theta}_0' \left(\tilde{\tau} + \frac{1}{2}\right) \pm_\Delta \Delta\tau K \left[\frac{4c\left(g - K_1\right) - K_1\tilde{\tau} + 2\left(g - 2K_1\right)\tilde{\tau}^2}{4K_2} - \frac{c\left(2 - 5c\Delta\tau^2\right)}{2K_2^{3/2}} \tilde{\tau} g_2 \right] ,$$

with

$$2K_1 = \sqrt{1 - 2c\left(1 - 2c\right)\Delta\tau^2} , \quad K_2 = 1 - 2c\Delta\tau^2 ,$$

$$g = \sqrt{c^2\Delta\tau^2 + \left(1 - 2c\Delta\tau^2\right)\tilde{\tau}^2} , \quad g_2 = \log\left[\frac{g\sqrt{K_2} + \left(1 - 2c\Delta\tau^2\right)\tilde{\tau}}{-1/2 + c\Delta\tau^2 + K_1\sqrt{K_2}} \right] .$$

The boundary conditions given by Eq.(21) can now be imposed. The radial velocity automatically satisfies them due to symmetries, while for the radial position and transversal velocity one reaches

(after several algebraic manipulations):

$$\begin{aligned} \left(4 - 7c\Delta\tau^2\right) &= 2KK_1\,, \\ \sqrt{K_2} &= 2cK \log \frac{2K_1 + \sqrt{K_2}}{2K_1 - \sqrt{K_2}}\,. \end{aligned} \tag{29}$$

This nonlinear system can be solved numerically for the values of $\Delta\tau$ and c. Interestingly, by taking the limit $c \to 0$ it reduces to the results already obtained for the bang-bang control, with the first equation returning the same estimate for $\Delta\tau$ as Eq. (27) and the second one becoming incompatible (because it is not possible to fulfill all the boundary conditions without introducing c). The second part of Eq. (29) is not easy to handle (even numerically, since the logarithmic term is close to an indetermination of the type $0 \cdot \infty$ for $\Delta\tau \to 0$), but the first one turns out to be a polynomial both in c (second degree) and $\Delta\tau$ (sixth degree with only even powers):

$$16\chi^2 - 56c\chi^2\Delta\tau^2 + \left(-1 + 49c^2\chi^2\right)\Delta\tau^4 + 2c\,(1 - 2c)\,\Delta\tau^6 = 0\,.$$

The roots of this polynomial can be found analytically either for c or $\Delta\tau$. The full solution for $\Delta\tau$ is too lengthy to report here, but by retaining terms up to order 4 in $\Delta\tau$ a first approximation is found in a compact way:

$$\Delta\tau \approx \frac{2\sqrt{\chi}}{\sqrt{1 + 7\chi c}}\,, \tag{30}$$

This shows that the influence of c on the time of flight is small, being scaled by $\chi \ll 1$. On the other hand, the solution for c would take the following form:

$$c = \frac{-28\chi^2 + \Delta\tau^4 + \Delta\tau\sqrt{\chi^2\,(64 - 7\Delta\tau^2) + \Delta\tau^4\,(-4 + \Delta\tau^2)}}{-49\chi^2\Delta\tau^2 + 4\Delta\tau^4}\,,$$

which goes to 0 as $\Delta\tau$ approaches $2\sqrt{\chi}$.

Once $\Delta\tau$ and c are determined, the new value for $\hat{A}$ can be recovered by introducing the expansions for $\hat{\lambda}_u$ and $\hat{\lambda}_v$ into the transversality condition, Eq. (20), and retaining terms up to order 4 in $\Delta\tau$, yielding:

$$\hat{A} \approx \pm_\Delta \frac{2}{\Delta\tau\sqrt{1 + \Delta\tau^2\,(1/6 - 2c + 4c^2)}}\,,$$

whereas $\hat{C}$ is obtained from the definition of c, Eq. (28):

$$\hat{C} \approx \hat{A}\left(c\Delta\tau^2 - 2\right)\,.$$

Although this new control improves the solution for Eqs. (25) and (26), fulfilling all the boundary conditions, its validity as a solution for the linear formulation is still limited by the fact that small terms for $\Delta\tau \ll 1$ have been neglected in the equations of motion. Furthermore, during the definition of the control vector it was assumed that terms of order 4 and higher in $\Delta\tau$ where negligible in the expansion for $\lambda_u^2 + \lambda_v^2$. However, a closer look reveals that the quadratic term is scaled by $K_2 = 1 - 2c\Delta\tau^2$, which goes to zero as χ increases, whereas the coefficient for the quartic term grows with $\Delta\tau^2$. Therefore, the series expansion used to approximate u_ρ and u_θ breaks down for high enough values of χ, further limiting the applicability of this solution for $\chi \sim 1$.

Similarly to the work by Broucke [2], an analytical description of the costates for the linearized problem has been reached. The main advantage of the proposed method is that it does not require the numerical evaluation of additional parameters (at least for the first approximation).

B. Long-maneuver regime

In the long-maneuver regime, since $\Delta\tau \gg 1$ from Eq. (22) it follows that:

$$\left|\hat{\lambda}_u\right| \leq \left|\hat{A}\right| , \quad \left|\hat{\lambda}_v\right| \leq 2\left|\hat{A}\right| + \left|\hat{C}\right| ,$$

and the requirement of $|u_\theta| \sim 1$ (i.e. $|\hat{\lambda}_v| \gg |\hat{\lambda}_u|$) leads to:

$$\left|\hat{C}\right| \gg \left|\hat{A}\right| .$$

Introducing this into the transversality condition, Eq. (15), and retaining only the leading terms yields an estimation for $\hat{C}$:

$$\hat{C} \approx \pm 1 ,$$

while for $\hat{A}$ only the bound:

$$\left|\hat{A}\right| \ll 1 ,$$

is available. Gathering these results, the dominant component of the primer vector can now be approximated as:

$$\hat{\lambda}_v \approx \pm 1 ,$$

showing that, contrary to the short-maneuver regime, there is no reversal in the direction of thrust during the maneuver.

The equations of motion can be approximately solved by neglecting the non-dominant terms and assuming $|u_\theta| = 1$, leading to:

$$2\Delta\tau\hat{\theta}' + 3\Delta\tau^2\hat{\rho} \approx 0\,,$$

$$\hat{\theta}'' + 2\Delta\tau\hat{\rho}' \approx K u_\theta\,.$$

The first equation provides a relation between the radial displacement and the angular velocity, and substituting it into the second equation leads to a system of first order ODEs:

$$\begin{aligned} \hat{\theta}' &\approx -\frac{3}{2}\Delta\tau\hat{\rho}\,, \\ \hat{\rho}' &\approx 2\frac{\Delta\tau}{\chi}u_\theta\,. \end{aligned} \tag{31}$$

The second of Eq. (31) shows that u_θ has to be positive for $\Delta\rho > 0$, allowing to determine the signs for the transversal component of the primer vector:

$$\hat{\lambda}_v \approx \mp_\Delta 1\,, \quad \hat{C} \approx \mp_\Delta 1\,.$$

Eq. (31) can now be readily integrated to yield:

$$\hat{\rho} - \hat{\rho}_0 \approx \pm_\Delta 2\frac{\Delta\tau}{\chi}\hat{\tau}\,,$$

$$\hat{\theta} - \hat{\theta}_0 \approx \frac{3}{2}\Delta\tau\left(\mp_\Delta\frac{\Delta\tau}{\chi}\hat{\tau}^2 - \hat{\rho}_0\hat{\tau}\right)\,,$$

and imposing $\Delta\hat{\rho} = \pm_\Delta 1$ gives an estimate for the time of flight:

$$\Delta\tau \approx \frac{\chi}{2}\,. \tag{32}$$

Note that this expression has a different structure from the one obtained for the short-maneuver regime, Eq. (27). However, there is not an inconsistency with the units as both $\Delta\tau$ and χ are non-dimensional parameters.

Since the linearized equations of motion have been reduced to a first order system by neglecting small terms, only the initial conditions for $\hat{\rho}$ and $\hat{\theta}$ can be directly imposed. Interestingly, it is straightforward to check that $\hat{\theta}'$ also fulfills its initial condition, whereas $\hat{\rho}'$ is constant and can never

meet either of its boundary conditions. This shows that the small components in the linearized equations of motion, particularly the radial contribution of the thrust acceleration, have to be retained in order to impose all the boundary conditions.

A more accurate solution is now sought for by defining an approximation for the control vector that includes the small contribution of its radial component. After some manipulations it is possible to write u_ρ and u_θ in the form:

$$u_\rho = \pm_\Delta \frac{\overline{A}\sin\left(\Delta\tau\tilde{\tau}\right)}{\sqrt{1+4\overline{A}\cos\Delta\tau\tilde{\tau}+\frac{1}{2}\overline{A}^2\cos 2\Delta\tau\tilde{\tau}}}\,,$$

$$u_\theta = \pm_\Delta \frac{1+2\overline{A}\cos\left(\Delta\tau\tilde{\tau}\right)}{\sqrt{1+4\overline{A}\cos\Delta\tau\tilde{\tau}+\frac{1}{2}\overline{A}^2\cos 2\Delta\tau\tilde{\tau}}}\,,$$

where $\overline{A} = \hat{A}/\hat{C}$. Since $|\hat{A}| \ll |\hat{C}|$, it is possible to expand the previous expressions for $|\overline{A}| \ll 1$ to reach:

$$u_\rho = \pm_\Delta \left[\overline{A}\sin\left(\Delta\tau\tilde{\tau}\right) - \overline{A}^2\sin\left(2\Delta\tau\tilde{\tau}\right) + \mathcal{O}\left(\overline{A}^3\right)\right]\,,$$

$$u_\theta = \pm_\Delta \left[1 - \frac{1}{4}\overline{A}^2 - \frac{1}{4}\overline{A}^2\cos\left(2\Delta\tau\tilde{\tau}\right) + \mathcal{O}\left(\overline{A}^3\right)\right]\,.$$

Higher time harmonics appear as more terms in $\overline{A}$ are retained, but their contribution is small because $\overline{A} \ll 1$. From now on only the first harmonic is considered, leading to:

$$u_\rho \approx \pm_\Delta \overline{A}\sin\left(\Delta\tau\tilde{\tau}\right) = \pm_\Delta \overline{A}\sin\Delta\tau\left(\hat{\tau}-1/2\right)\,,\quad u_\theta \approx \pm_\Delta \overline{C}\,, \tag{33}$$

where:

$$\overline{C} = 1 - \frac{1}{4}\overline{A}^2\,, \tag{34}$$

and $\overline{A}$ corresponds to the amplitude of the control vector oscillations about the transversal direction.

The full linearized equations of motion, Eq. (5), can be solved analytically for the periodic control vector in Eq. (33) and the initial conditions given by Eq. (21) to reach:

$$\hat{\rho}' = \pm_\Delta 2\frac{\Delta\tau}{\chi}\left[\left(\Delta\tau\frac{\overline{A}}{4}\sin\Delta\tau\left(\hat{\tau}-1/2\right)\right)\hat{\tau} + \overline{C}\left(1-\cos\Delta\tau\hat{\tau}\right) - \frac{\overline{A}}{4}\sin\frac{\Delta\tau}{2}\sin\Delta\tau\hat{\tau}\right]\,,$$

$$\hat{\rho} - \hat{\rho}_0 = \pm_\Delta 2\frac{\Delta\tau}{\chi}\left[\left(\overline{C} - \frac{\overline{A}}{4}\cos\Delta\tau\left(\hat{\tau}-1/2\right)\right)\hat{\tau} + \left(-\overline{C} + \frac{\overline{A}}{4}\cos\frac{\Delta\tau}{2}\right)\frac{\sin\Delta\tau\hat{\tau}}{\Delta\tau}\right]\,,$$

$$\hat{\theta}' - \hat{\theta}'_0 = \pm_\Delta \frac{\Delta\tau}{\chi}\left[\left(4\overline{C} - \overline{A}\cos\frac{\Delta\tau}{2}\right)\sin\Delta\tau\hat{\tau} + \Delta\tau\left(-3\overline{C} + \overline{A}\cos\Delta\tau\left(\hat{\tau} - 1/2\right)\right)\hat{\tau}\right],$$

$$\hat{\theta} - \hat{\theta}_0 = \hat{\theta}'_0\hat{\tau} \pm_\Delta \frac{\Delta\tau}{\chi}\left[-\frac{3}{2}\Delta\tau\overline{C}\hat{\tau}^2 + \left(\overline{A}\sin\Delta\tau\left(\hat{\tau} - 1/2\right)\right)\hat{\tau}\right.$$
$$\left. + \left(4\frac{\overline{C}}{\Delta\tau} - 2\frac{\overline{A}}{\Delta\tau}\cos\frac{\Delta\tau}{2}\right)\left(1 - \cos\Delta\tau\hat{\tau}\right) + \frac{\overline{A}}{\Delta\tau}\sin\frac{\Delta\tau}{2}\sin\Delta\tau\hat{\tau}\right].$$

The boundary conditions at $\hat{\tau} = 1$, Eq. (21), can now be imposed:

$$\hat{\rho}'_f = 0 = \pm_\Delta 2\frac{\Delta\tau}{\chi}\left[\overline{C}\left(1 - \cos\Delta\tau\right) - \frac{\overline{A}}{4}\sin\frac{\Delta\tau}{2}\left(\sin\Delta\tau - \Delta\tau\right)\right],$$

$$\hat{\rho}_f - \hat{\rho}'_0 = \pm_\Delta 1 = \pm_\Delta\left[2\frac{\Delta\tau}{\chi}\left(\overline{C} - \frac{\overline{A}}{4}\cos\frac{\Delta\tau}{2}\right)\left(1 - \frac{\sin\Delta\tau}{\Delta\tau}\right)\right],$$

$$\hat{\theta}'_f - \hat{\theta}'_0 = \mp_\Delta\frac{3}{2}\Delta\tau = \pm_\Delta\frac{\Delta\tau}{\chi}\left[\overline{C}\Delta\tau - 4\Delta\tau\left(\overline{C} - \frac{\overline{A}}{4}\cos\frac{\Delta\tau}{2}\right)\left(1 - \frac{\sin\Delta\tau}{\Delta\tau}\right)\right].$$

Note that the solution for this system of equations does not depend on the sign of $\Delta\rho$. From the second equation it is possible to obtain an expression for $\overline{A}$ as a function of $\Delta\tau$ and $\overline{C}$:

$$\overline{A} = 8\overline{C}\frac{\sin\frac{\Delta\tau}{2}}{\sin\Delta\tau - \Delta\tau}. \tag{35}$$

Introducing Eq. (35) into the other two boundary conditions and operating, it turns out that both yield the same relation between $\Delta\tau$ and $\overline{C}$:

$$\Delta\tau = \frac{\chi}{2\overline{C}}. \tag{36}$$

Eqs. (34), (35), and (36) form a system of transcendental algebraic equations allowing to determine $\overline{A}$, $\overline{C}$, and $\Delta\tau$ for a given value of χ. It is observed that the time of flight estimate in Eq. (36) is a generalization of the one given by Eq. (32), which corresponded to $\overline{C} = 1$, showing that the time of flight increases slightly with the amplitude on the control oscillations. Regarding said amplitude, Eq. (35) reveals two important characteristics of its evolution with $\Delta\tau$. First of all, its average value decreases with the time of flight, so longer maneuvers have their control vector closer to the transversal direction. Secondly, the amplitude also depends on the time synchronization of the maneuver with respect to the orbital period of the reference orbit through the sine in the numerator. Maneuvers which take nearly a whole number of orbital revolutions of the reference to complete will have a lower amplitude of the control vector oscillation, thus being more efficient. Particularly,

Eq. (35) predicts no oscillations for $\Delta\tau = 2n\pi$ with $n \in \mathbb{N}$, although this will not happen in the actual trajectory due to the contribution of nonlinear terms.

The values of $\hat{A}$ and $\hat{C}$ can be calculated from $\overline{A}$, $\Delta\tau$ and the transversality condition. Substituting $\hat{A} = \overline{A}\hat{C}$ in Eq. (15) and solving for $\hat{C}$ yields:

$$\hat{C} = \mp_{\Delta} \sqrt{\frac{2}{2 + 5\overline{A}^2 + 8\overline{A}\cos\Delta\tau/2 + 3\overline{A}^2\cos\Delta\tau}}\,,$$

and then $\hat{A}$ can be directly obtained as $\overline{A}\hat{C}$.

Comparing this approach with the classic solution by Edelbaum [1], one can see that both have a similar complexity when just evaluating the first approximation for the time of flight. The computational cost of the new method increases when going into the refined approximation, but it has the advantage of capturing a more detailed description of the evolution of $\Delta\tau$ with the total displacement. Furthermore, it also provides detailed estimates for the states and costates, that can be used to initialize numerical resolution methods. On the other hand, Edelbaum's methods retains the nonlinearity of dynamics, and does not require the choice of a reference orbit. These two topics are reviewed in details in Sections III D and III E.

C. Transition Zone

As previously stated, it is not feasible to search for an analytical solution, even approximate, in the region between both limit regimes. In this transition zone the structure of the optimal maneuver undergoes fundamental qualitative and quantitative changes, as it evolves from the nearly bang-bang control profile of the short-maneuver regime to the nearly tangential control of the long-maneuver regime. It is however possible to predict for which values of the fundamental parameter χ it will developed by comparing the time of flight predictions obtained for the two limit regimes. Equating the time of flight estimates given by Eqs. (27) and (32) and solving for χ yields:

$$\chi \approx 16\,,$$

corresponding to a time of flight of

$$\Delta\tau \approx 8\,,$$

which is very close to the 2π period of the reference orbit. This is consistent with the previous conclusion that all the contributions in the equations of motion become of comparable order for $\Delta\tau \sim \mathcal{O}(1)$, and reinforces the idea that the main difference between both regimes is whether the maneuver takes less or more than one revolution of the reference orbit to complete.

The behavior in this transition zone is studied numerically through a set of test cases in the last section of the paper.

D. Nonlinearity effects

The developments in the previous sections are restricted to the linear formulation. Therefore, even the solution for the long-maneuver regime, which is feasible and near-optimal, will separate from the actual solution due to the contribution of nonlinear terms.

A time of flight estimate for the long-maneuver regime including the nonlinearity effects can be obtained leveraging the result that thrust orientation must be nearly tangential, and assuming quasi circular orbit during the transfer. Let us consider the vis-viva equation:

$$E = \frac{v^2}{2} - \frac{1}{1+\rho} = -\frac{1}{2a}\,, \tag{37}$$

where E is the specific energy, a is the semi-mayor axis, and v the velocity (all dimensionless). Deriving with respect to τ a relation between the derivatives of E and a is reached:

$$\frac{\mathrm{d}E}{\mathrm{d}\tau} = \frac{1}{2a^2}\frac{\mathrm{d}a}{\mathrm{d}\tau}\,.$$

Because thrust is tangential the derivative of E amounts to εv. Furthermore, the quasi circular condition allows us to write $a \approx 1+\rho$, and from Eq. (37) an expression for v as a function of a is reached:

$$v \approx \frac{1}{\sqrt{a}}$$

Gathering these results an ODE for the time evolution of a is obtained as follows:

$$\frac{\mathrm{d}a}{\mathrm{d}\tau} \approx 2\varepsilon a^{3/2}\,.$$

Integrating between 0 and $\Delta\tau$ and solving for $\Delta\tau$ finally yields an approximation for the time of

flight:

$$\Delta\tau = \pm_\Delta \frac{1}{\varepsilon} \frac{\sqrt{a_f} - \sqrt{a_0}}{\sqrt{a_0 a_f}} = \pm_\Delta \frac{\chi}{\Delta r} \frac{\sqrt{a_f} - \sqrt{a_0}}{\sqrt{a_0 a_f}}\,, \tag{38}$$

where $a_f = 1+\rho_f$, $a_0 = 1+\rho_0$. This result coincides with the classic solution given by Edelbaum[1]. Unlike the solution for the linearized dynamics it is now not possible to explicitly impose the boundary conditions, although the quasi circular hypothesis implies that they will be approximately fulfilled as long as it holds. It is interesting to check that, by expanding for $\rho \ll 1$ and retaining only the leading term, the first linear estimate is recovered:

$$\Delta\tau = \pm_\Delta \frac{\chi}{\Delta r} \frac{\rho_f - \rho_0}{2} + \mathcal{O}\left(\rho^2\right) \approx \frac{\chi}{2}\,.$$

A quantitative accounting of the influence of the nonlinearity effects in the optimal maneuver can be seen in the test cases included in section IV.

E. Selection of reference orbit

Owing to the use of a linearized model for dynamics, the approximate analytic expressions obtained so far do not explicitly depend on the choice of the reference orbit. However, the agreement between their predictions and the exact solution is expected to depend on said reference. Particularly, because gravity is linearized around the reference orbit the approximate solution will overestimate or underestimate its contributions depending on R. In this subsection, a criterion for the selection of a reference orbit in order to minimize these effects and improve the accuracy of the prediction is proposed.

Let us consider a second reference orbit of radius $\overline{R}$. The new units of length and time are $\overline{R}$ and the inverse mean motion $\overline{\Omega}^{-1} = \sqrt{\overline{R}^3/\mu}$, respectively. For now on, all non-dimensional values expressed with respect to this second reference are denoted as $\bar{\cdot}$. The ratio of the units of time for both reference orbits is:

$$\frac{\overline{\Omega}^{-1}}{\Omega^{-1}} = \left(\frac{\overline{R}}{R}\right)^{3/2}\,,$$

depending only on the ratio of the reference radii, as the primary is the same in both cases. The relations between $\Delta\tau$, radius change, non-dimensional thrust parameter, and χ for both references

can be computed to be:

$$\Delta\tau = \left(\frac{\overline{R}}{R}\right)^{3/2} \Delta\overline{\tau}\,, \quad \Delta r = \frac{\overline{R}}{R}\Delta\overline{r} \quad \varepsilon = \left(\frac{\overline{R}}{R}\right)^{-2} \overline{\varepsilon}\,, \quad \chi = \left(\frac{\overline{R}}{R}\right)^{3} \overline{\chi}\,. \tag{39}$$

It is key to understand how the choice of the reference orbit affects the $\Delta\tau$ prediction, especially because R does not appear explicitly in Eq. (27) or Eq. (32). Taking the short-maneuver approximation, Eq. (27), in reference R and changing it to reference $\overline{R}$, one gets:

$$\Delta\tau = 2\sqrt{\chi} \Rightarrow \left(\frac{\overline{R}}{R}\right)^{3/2} \Delta\overline{\tau} = 2\sqrt{\left(\frac{\overline{R}}{R}\right)^{3} \overline{\chi}} \Rightarrow \Delta\overline{\tau} = 2\sqrt{\overline{\chi}}\,,$$

that is, the short-maneuver $\Delta\tau$ approximation is reference-independent. The same procedure applied to the long-maneuver case yields:

$$\Delta\tau = \frac{\chi}{2} \Rightarrow \left(\frac{\overline{R}}{R}\right)^{3/2} \Delta\overline{\tau} = \left(\frac{\overline{R}}{R}\right)^{3} \frac{\overline{\chi}}{2} \Rightarrow \Delta\overline{\tau} = \left(\frac{\overline{R}}{R}\right)^{3/2} \frac{\overline{\chi}}{2}\,,$$

which differs from the result obtained by applying Eq. (32) directly in reference $\overline{R}$. Therefore, the ToF estimate for the long-maneuver regime depends on the choice of the reference orbit. Note that the aim of this reasoning is just to identify the effects in $\Delta\tau$ of changing reference orbit; the proper way of computing it is still to apply the original formulas, as their derivation does not depend on the reference orbit.

Given that the short-maneuver ToF estimation is not affected by R, one criteria for the choice of the reference orbit would be to make the long-maneuver linearized time estimation match the averaged, nonlinear Edelbaum's solution, Eq. (38), which is known to be very accurate for multi-revolution transfers [1]. The new reference radius reads:

$$\overline{R} = \left[\frac{1}{2}\frac{\sqrt{A_0 A_f}\Delta R}{\left|\sqrt{A_f} - \sqrt{A_0}\right|}\right]^{2/3} = \left[\frac{1}{2}\sqrt{A_0 A_f}\left(\sqrt{A_0} + \sqrt{A_f}\right)\right]^{2/3}. \tag{40}$$

where A_0 and A_f are the dimensional values of the initial and final semimajor axis, and $\Delta R = |A_f - A_0|$. Alternatively, if the non-dimensional semimajor axis in reference R are given the ratio between $\overline{R}$ and R is:

$$\frac{\overline{R}}{R} = \left[\frac{1}{2}\sqrt{a_0 a_f}\left(\sqrt{a_0} + \sqrt{a_f}\right)\right]^{2/3}. \tag{41}$$

IV. Test Cases

The proposed minimum-time transfer is now solved numerically for several Earth-bound and interplanetary test cases. Wide ranges are considered for the dimensionless thrust parameter ε and the radial displacement Δr. Although some of these values may lack a practical interest (for instance, having a thrust acceleration too high or requiring an exceedingly long time of flight), they serve to highlight the physical and mathematical characteristics of the problem and the differences between the linear and nonlinear cases. These numerical solutions are obtained solving the TPBVP derived from the indirect method in the previous sections. A different approach using a direct transcription and a large-scale NLP solver can be seen in previous works by Gonzalo et al.[16].

The TPBVP derived from the indirect method is solved using a classic shooting scheme. Keeping the assumption that all values of the initial and final states are fixed except for θ_f, the corresponding shooting function can be written as follows:

$$\mathbf{Z}\left(\boldsymbol{\lambda}_0, \Delta\tau\right) = \begin{bmatrix} \dot{\rho}\left(\Delta\tau\right) \\ \dot{\theta}\left(\Delta\tau\right) - \dot{\theta}_f \\ \rho\left(\Delta\tau\right) - \rho_f \\ \lambda_\theta\left(\Delta\tau\right) \\ H\left(\Delta\tau\right) \end{bmatrix} = \mathbf{0}\,,$$

where $\mathbf{S}\left(\Delta\tau\right)$ and $\boldsymbol{\lambda}\left(\Delta\tau\right)$ are obtained integrating Eqs. (4) and (13) (or Eqs. (5) and (17) for the linearized problem) with initial conditions $[\mathbf{S}_0\, \boldsymbol{\lambda}_0]$. The initial condition for the state, $\mathbf{S}_0$, is given by Eq. (6) (or Eq. (7) for the linearized case), whereas $\boldsymbol{\lambda}_0$ is an unknown of the shooting algorithm. Continuing with the definition of the shooting algorithm, it is important to note that the previous shooting function corresponds to a single-shooting scheme. The results presented in this work have been obtained using a multiple-shooting algorithm with 32 segments; that requires augmenting the vector of unknowns with the states and costates at the beginning of each intermediate segment as well as adding the equations for the matching of consecutive segments (8 extra unknowns and equations for each additional segment, leading to a total of 261 unknowns). In all cases, the reference orbit is either the initial, the final or the intermediate one (see Section III E), and the initial angular position is set to zero for simplicity.

Third party algorithms are employed both for integrating the system of ODEs (Matlab's *ode45*) and zero finding (Matlab's *fsolve* and its Trust-Region-Dogleg algorithm). In order to improve the robustness and efficiency of the method, the Jacobian for the shooting function is constructed analytically from the State Transition Matrix (STM) for $[\mathbf{S}^\top \boldsymbol{\lambda}^\top]$, following a procedure analogous to the one proposed by Zhang et al.[17] for the Cartesian case. Computing the STM requires to analytically derive the variational equation and integrating it alongside the ODE system for state and costate; because the STM is a 8×8 matrix for the planar problem in curvilinear coordinates, this means adding 64 ODEs to the problem (for a total of 72 ODEs). The derivation of the variational equation is relatively simple and can be performed using a symbolic manipulator.

One last aspect to consider is the generation of an initial guess of the solution for the iterative multiple shooting algorithm. For the linear case the refined versions of the analytical approximations are used except for a region around the transition zone corresponding to $\chi \in [6, 16]$, where the underlying hypothesis lose validity (as previously commented) and the first approximation is preferred. This approach proves to be remarkably good, allowing to solve all the linear test cases. For the nonlinear cases the corresponding linear solution is tried first, falling back to a continuation in χ if the shooting algorithm fails to converge. The linear solution proves to be a good enough initial guess for the short-maneuver regime in all the test cases, and also for the transition zone and long-maneuver regime in problems with small Δr (small contribution of the nonlinear terms).

Figure 2 shows the evolution of the maneuver time $\Delta\tau$ with χ for an orbit raise of 200 km departing from GEO (42164.1 km). Because the relative displacement is very small, $\Delta r = 4.7433\times10^{-3}$, the linear and nonlinear solutions are practically identical, and only the latter is included for clarity. The two different regimes predicted by the qualitative study of the equations can be clearly identified, with the transition between them taking place for values of $\Delta\tau$ around one orbit of the reference, that is, $\Delta\tau/2\pi \approx 1$. This supports the hypothesis that one of the key differences between both regimes is whether the maneuver can be completed in one revolution of the reference orbit or not. The figure also represents the different approximations of $\Delta\tau$ previously obtained for the short- and long-maneuver regimes, showing a great correspondence with the numerical results. Both the first and refined approximations remain very close to the exact solution except for a small region

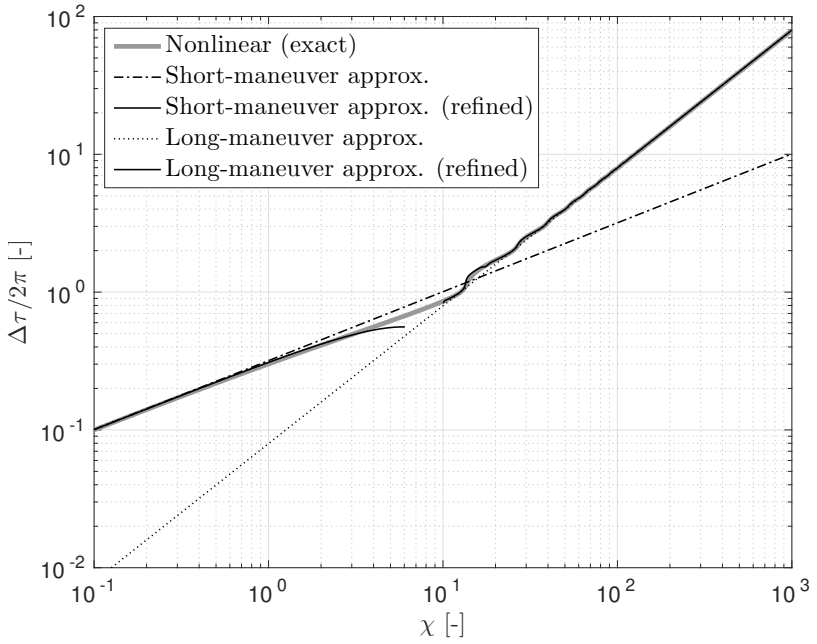

Fig. 2 Time of flight as a function of χ for an orbit raise of 200 km departing from GEO (initial orbit is taken as reference).

corresponding to the transition zone. It is interesting to note how the refined approximation for the long-maneuver regime holds even for values of χ corresponding to less than one revolution of the reference orbit (inside the transition zone), whereas the refined approximation for the short-maneuver regime diverges rapidly as the transition zone is approached. This breakdown of the refined short-maneuver approximation was already predicted from the equations, because some of the hypothesis used for its derivation lose validity as the time of flight approaches one revolution. Focusing again on the long-maneuver regime, the oscillations in $\Delta\tau$ predicted by the refined approximation can be clearly identified, with the first approximation corresponding to the secular behavior.

The effect of nonlinearities can be clearly appreciated in Figure 3, corresponding to two LEO to LEO transfers with the same arrival orbit at an altitude of 650 km. The altitudes of the departure orbits are 850 km and 1400 km, corresponding to $\Delta r = 2.7670\times10^{-2}$ and 9.6424×10^{-2}, respectively. As expected, the higher the value of Δr the more the exact solution separates from the linear one (common to both cases) due to the nonlinear contributions. However, this separation only appears in the transition zone and the long-maneuver regime, whereas both solutions remain close to the linear case for the short-maneuver regime. This is due to the nonlinear effects not having enough

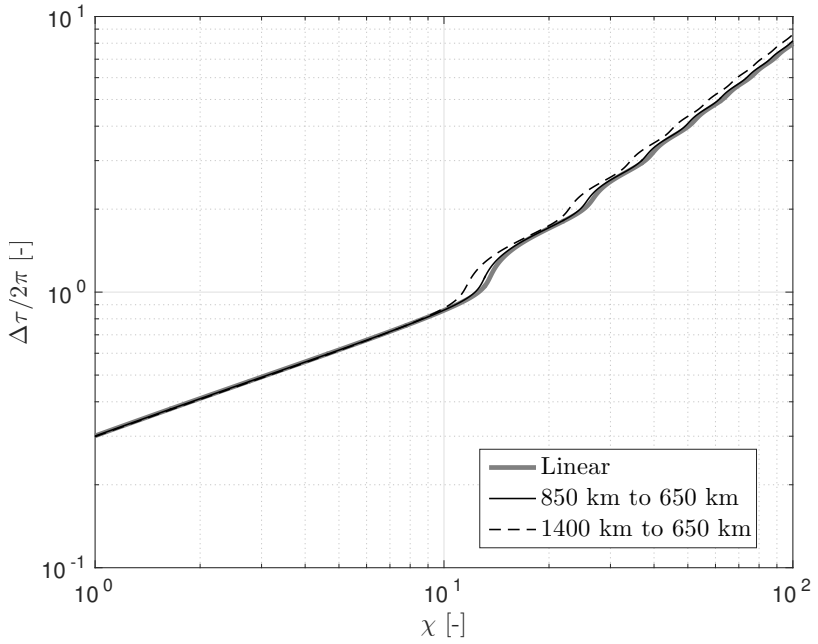

Fig. 3 Time of flight as a function of χ for two LEO to LEO transfers (the final orbit is taken as reference). Note that the linear solution is common to all cases.

Table 1 Data for the interplanetary test cases. Orbits are assumed to be circular and coplanar, and all transfers depart from Earth's orbit. Orbital radii are taken from [18] and [19].

Body	Radius [10^6 km]	Δr [–]
Mercury	57.91	0.6130
Venus	108.21	0.2767
Earth	149.60	–
Mars	227.92	0.5235
Ceres	414.09	1.7680
Jupiter	778.57	0.8078
Saturn	1433.53	8.5824
Uranus	2872.46	18.2009

time to fully develop for transfers in the short-maneuver regime, characterized by relatively shorter transfer times.

The previous conclusions about the effect of nonlinearities are reinforced by the results obtained in Figure 4 for several interplanetary test cases. All departure and arrival orbits are coplanar and circular, with radii corresponding to the semimajor axis of several planets and an asteroid in the

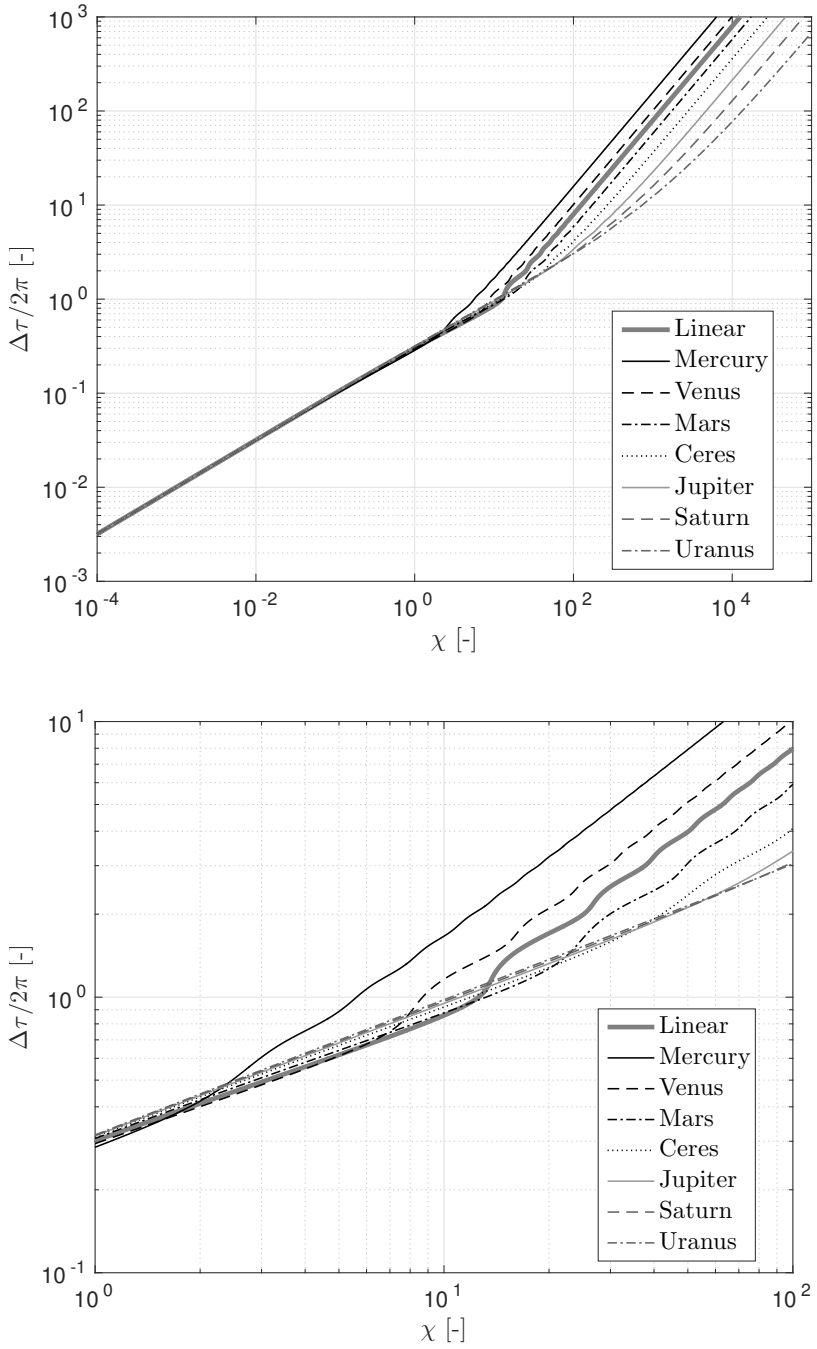

Fig. 4 Time of flight as a function of χ for several interplanetary test cases departing from Earth (Earth's orbit is taken as reference). The curve for each planet corresponds to the exact nonlinear solution, whereas the linear one is common to all cases.

Solar System as reported in Table 1. In all cases, the departure orbit is the one corresponding to Earth, which is also taken as reference. The results show that the separation between the linear and nonlinear solutions grows with Δr, with negative radial variations increasing the time of flight

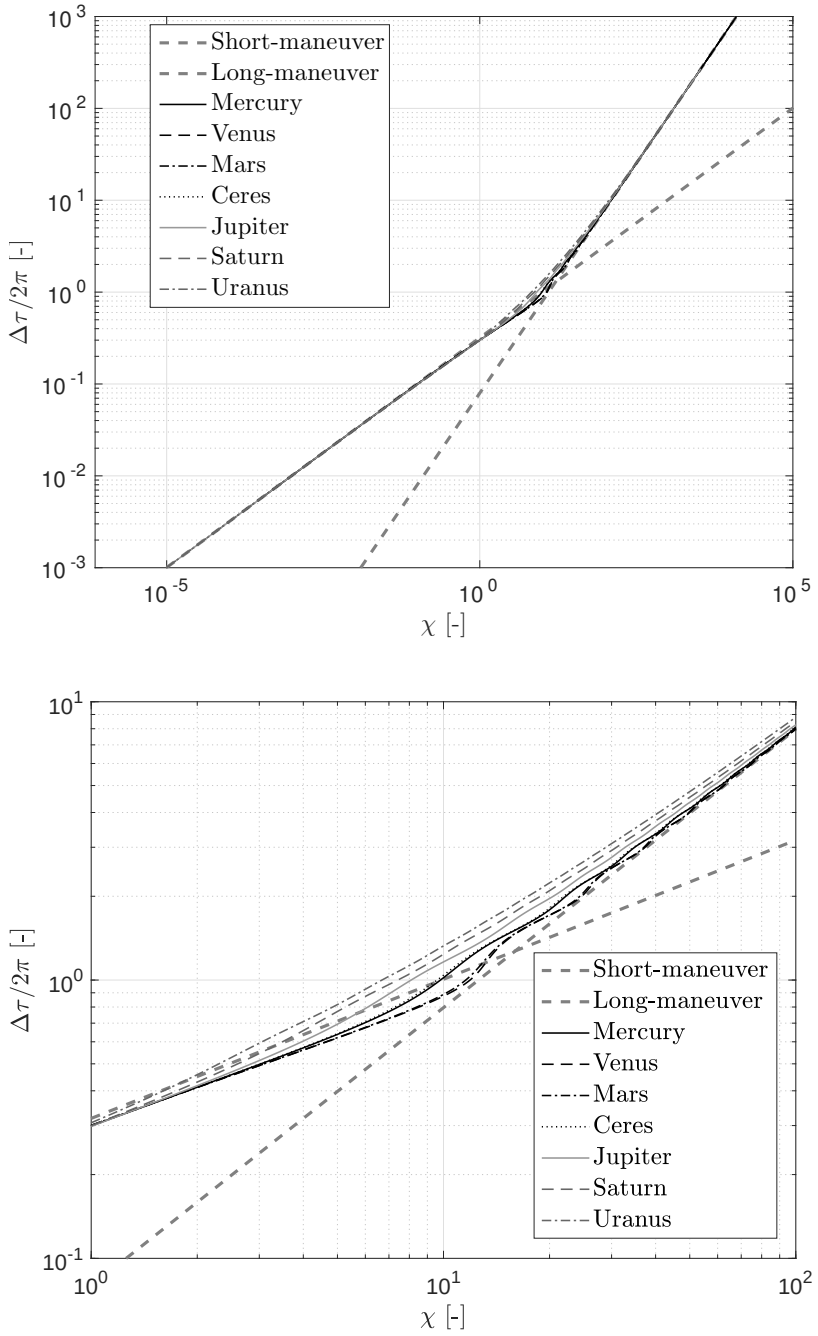

Fig. 5 Time of flight as a function of χ for several interplanetary test cases departing from Earth (each case has a different reference orbit, determined following the procedure in Section III E). The curve for each planet corresponds to the exact nonlinear solution, whereas the linear one is common to all cases.

for a given χ and positive radial variations decreasing it. Additionally, the oscillations in $\Delta\tau$ for the long-maneuver regime decrease as Δr increases, completely disappearing in the Saturn an Uranus

examples. Furthermore, it is also observed that those cases present a larger transition zone until the long-maneuver asymptotic evolution of $\Delta\tau$ is reached.

A clear takeaway from Fig. 4 is that the linear solution underestimates $\Delta\tau$ when the radius of the final orbit is smaller than that of the reference, and overestimates it when the final orbit is larger. This effect can be removed by setting an intermediate reference orbit radius for each test case using Eq. (40). Figure 5 shows the results for the same interplanetary transfers as Fig. 4, each one expressed in its corresponding intermediate reference orbit (note that it changes from curve to curve). One can notice that this choice for the reference orbit causes all the curves to collapse together, except for some differences in the transition zone. However, this change of reference orbit does not improve the performance of the linear solution as initial guess for the nonlinear one, as the qualitative changes between both remain (especially in the transition regime or under strong nonlinearities). That means that it is not advisable to refer to an intermediate orbit when implementing a numerical optimization scheme.

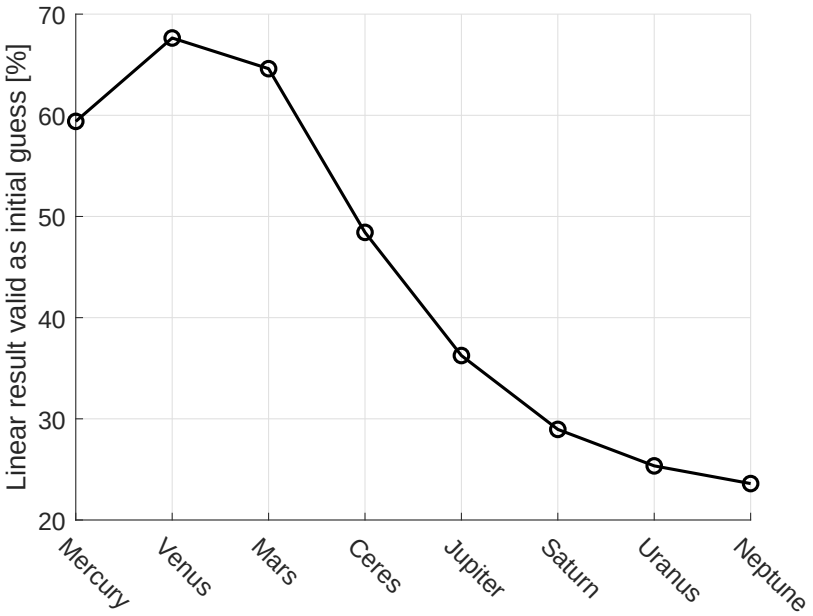

Fig. 6 Percentaje of cases for each interplanetary transfer for which the linear solution worked as initial guess for the nonlinear one.

The validity of the linear solution as initial guess for the nonlinear case is characterized in Figs. 6 and 7. The former shows how the number of cases that can be solved using the initial solution as

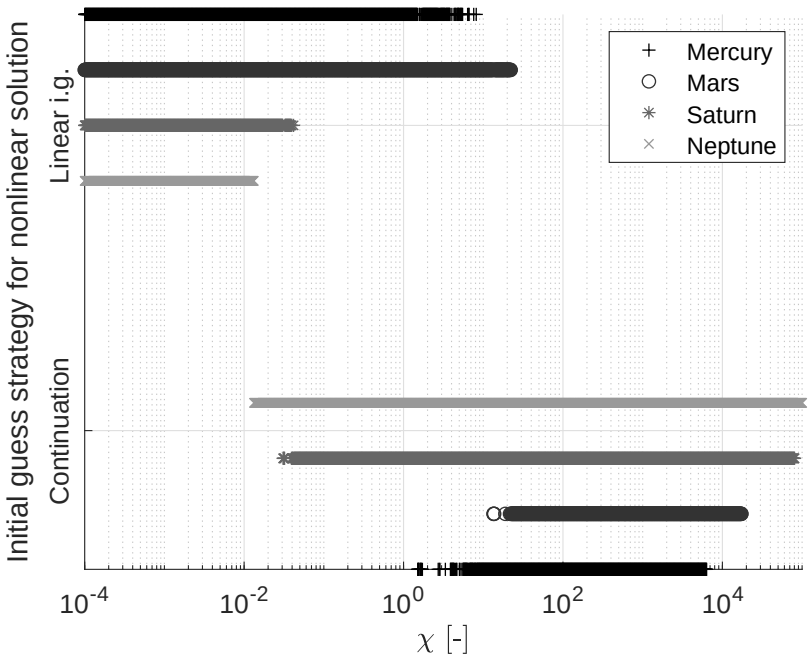

Fig. 7 Sucesfull initial guess strategy for the nonlinear solution as a function of χ, for several interplanetary transfers.

initial guess decrease with the separation between the initial and final planets, which corresponds to stronger nonlinearities. On the other hand, the results in Fig. 7 for four different transfers reveal that the linear solution is always a good initial guess in the short-maneuver regime, with the first failed cases appearing close to the transition zone (and the sooner the higher the nonlinearities).

More detailed information for the Earth-Mars case including the time estimates is given in Figure 8. The refined long-maneuver approximation perfectly reproduces the time of flight for the linear solution, but both separate appreciably from the exact solution due to the effect of the nonlinearities. On the other hand, the $\Delta\tau$ estimate by Edelbaum, which is based on the nonlinear equations, properly captures the secular behavior but fails to reproduce the small oscillations. Interestingly, the first long-maneuver approximation and the Edelbaum's solution are parallel lines in logarithmic scale.

Figures 10-12 present three representative cases taken from both regimes and the transition zone, for the Earth-Mars test case using Earth's orbit as reference. The qualitative features shown for each regime are common to all test cases, keeping in mind that the separation between the linear and nonlinear solution increases with Δr. Figure 10 shows the thrust orientation angle, curvilinear

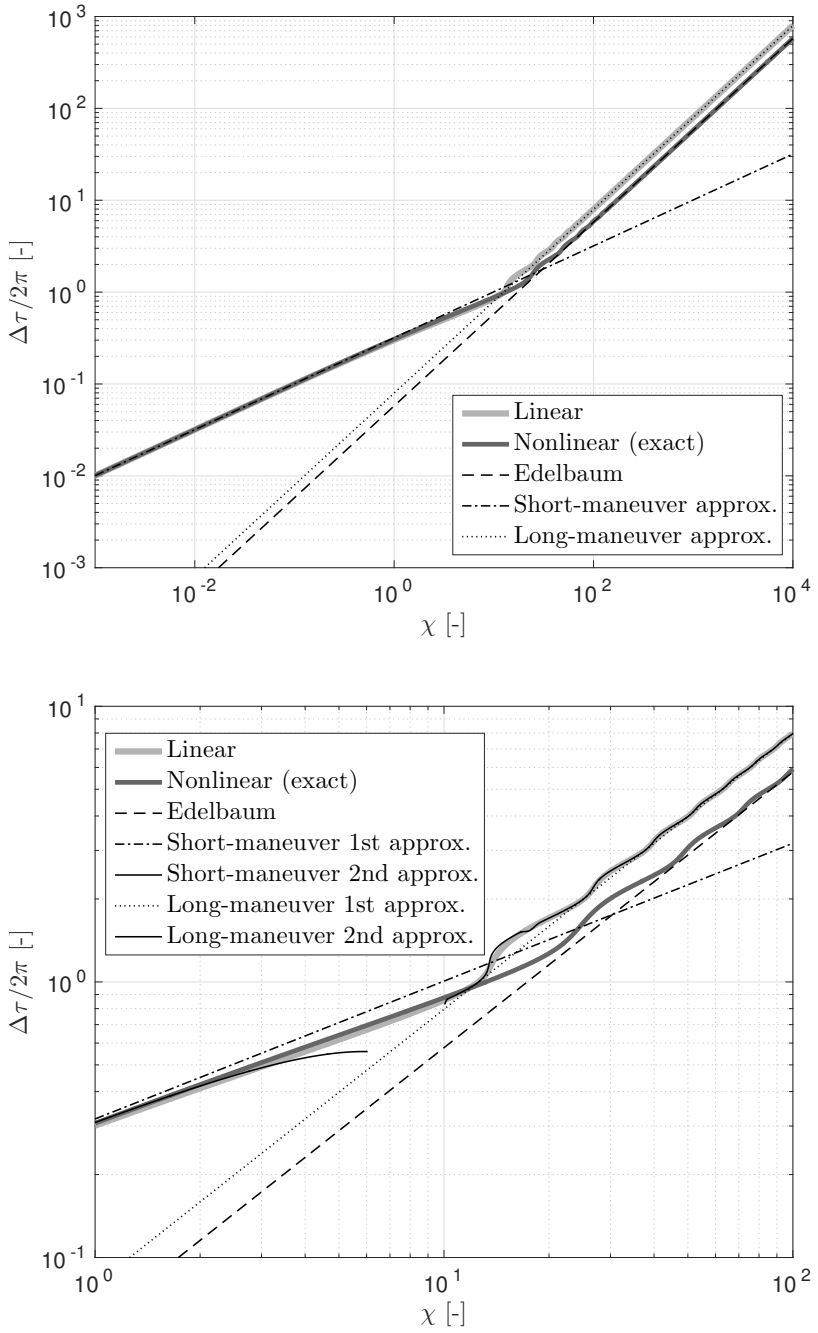

Fig. 8 Time of flight as a function of χ for the Earth to Mars test case (Earth's orbit is taken as reference). Curves corresponding to the time of flight estimations for the short and long-maneuver regimes, as well as the classic solution by Edelbaum, are included.

position and costate of the velocity for a transfer in the short-maneuver regime, with $\chi = 0.2405$ and a dimensionless thrust acceleration of 2.1764. Times of flight are 0.9644 for the linear solution and 0.9619 for the exact one (corresponding to 0.1534 and 0.1530 revolutions of the reference orbit,

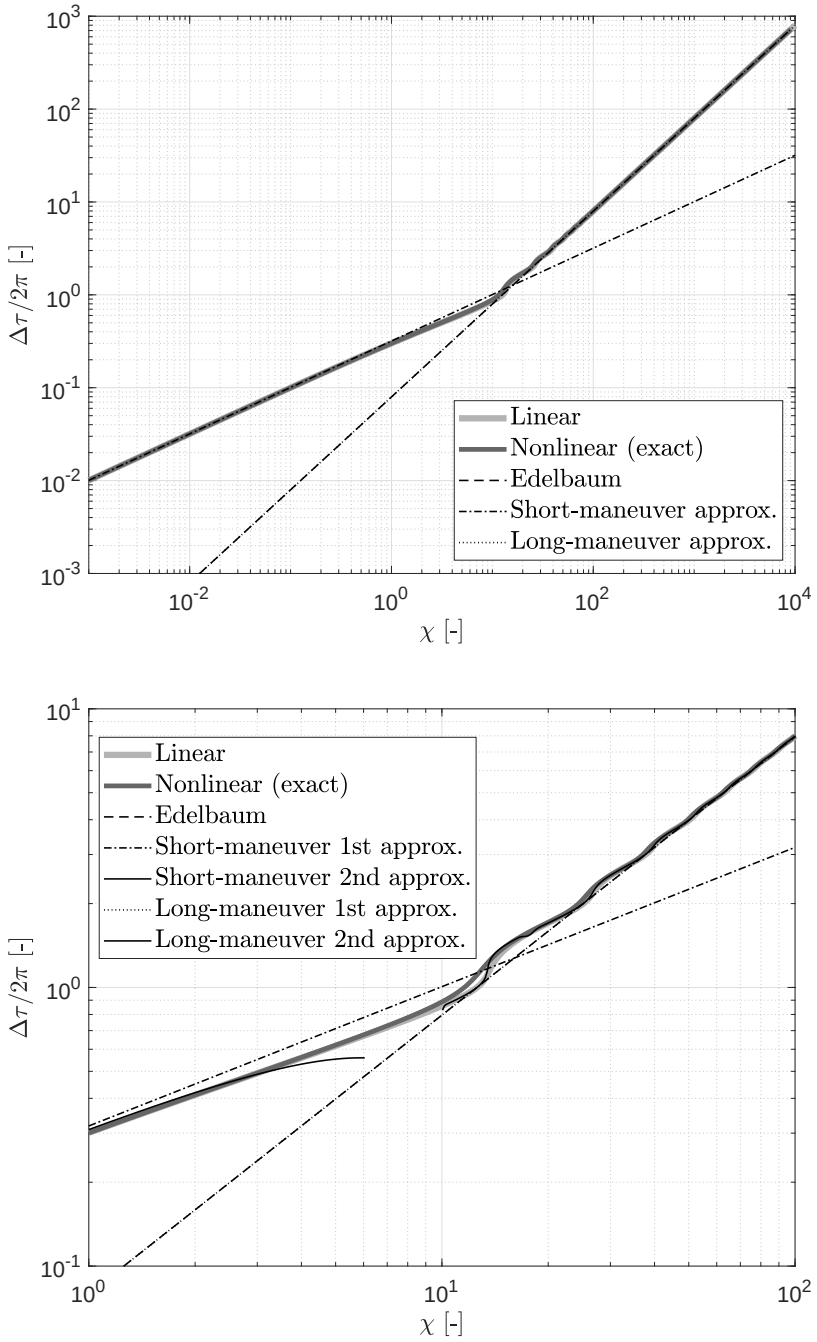

Fig. 9 Time of flight as a function of χ for the Earth to Mars test case (with intermediate reference orbit as defined in Section III E). Curves corresponding to the time of flight estimations for the short and long-maneuver regimes, as well as the classic solution by Edelbaum, are included.

respectively). The control variable γ resembles a bang-bang control as predicted, with the switch located at the middle of the maneuver. Thrust is oriented close to the positive radial direction

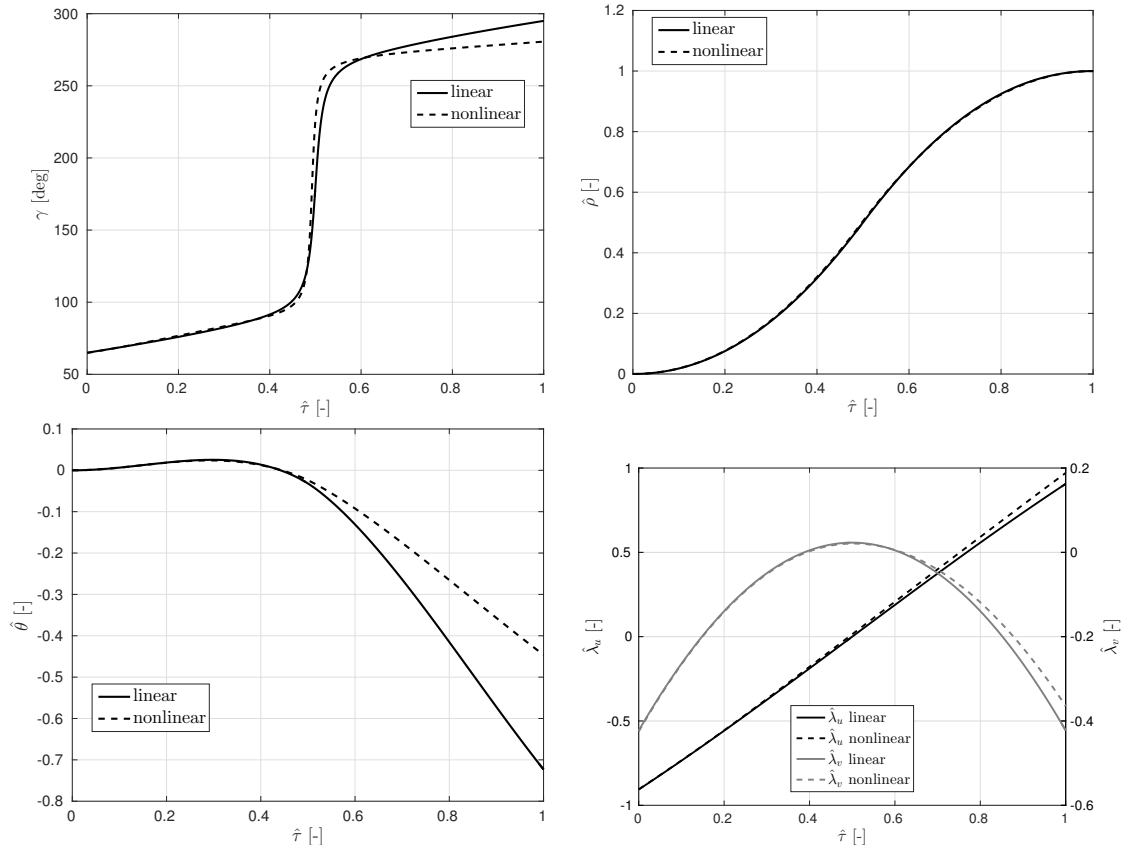

Fig. 10 Earth to Mars transfer for a non-dimensional thrust acceleration of 2.1764 **(corresponding to** $\chi = 0.2405$**).**

during the first half of the maneuver, and in the second half it reverses to point opposite to it. Interestingly, the linear and nonlinear γ profiles are very similar at the beginning but appreciably separate towards the end of the transfer. This is also reflected in the curves for the costate elements involved in the control equation, $\hat{\lambda}_u$ and $\hat{\lambda}_v$. However, the most notable differences are observed in the final values of the angular position. The main reason behind this is the different value of the boundary condition for the final angular velocity for the linear and nonlinear problems. On the other hand, the profiles for the radial position are almost identical in both cases. In general, the linear solution for γ, $\hat{\rho}$ and the costates fit very well with the behaviors predicted by the approximate analytic solutions. Also noteworthy is that the symmetry properties of the linear solution are not preserved for the complete nonlinear model.

The solution has a completely different structure in the long-maneuver regime, as shown in Figure 11 for $\chi = 1.2869{\times}10^2$ and a dimensionless thrust acceleration of $4.0680{\times}10^{-3}$. Time of flight

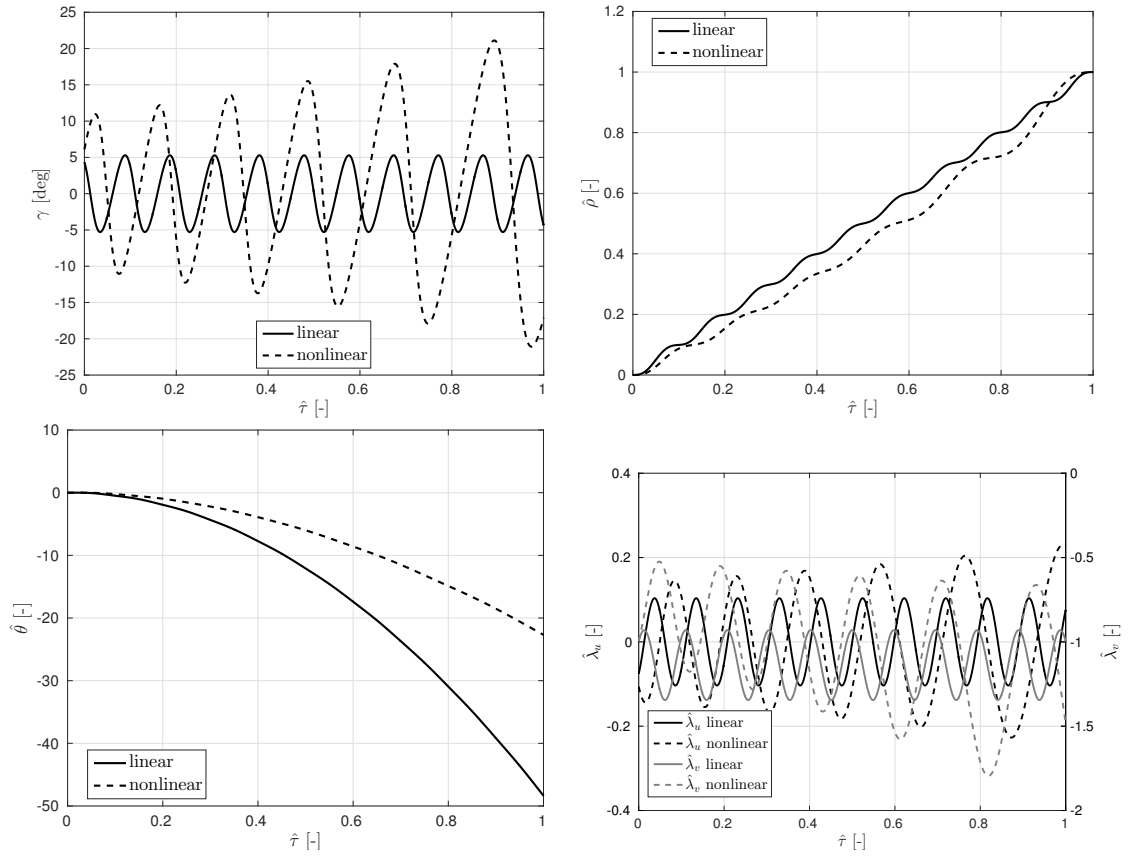

Fig. 11 Earth to Mars transfer for a non-dimensional thrust acceleration of 4.0680×10^{-3} **(corresponding to** $\chi = 1.2869\times10^{2}$**).**

is 64.4812 for the linear case and 47.3139 for the nonlinear one (10.2625 and 7.5302 revolutions of the reference orbit, respectively). Contrary to the short-maneuver example, the separation between the linear and complete models due to the effect of the nonlinearities is clearly observed in all variables. The thrust control angle is now oriented along the transversal direction, describing small oscillations about it both in the linear and nonlinear cases. However, the amplitude of the oscillations in the linear solution is constant, whereas for the exact model it increases with time. Similar oscillatory behaviors can also be found for the rest of variables, except for $\hat{\theta}$. Interestingly, the secular evolution of $\hat{\rho}$ has changed from quadratic to linear, justifying the different slopes showed in Figure 8 for $\Delta\tau\,(\chi)$. Same as with the short-maneuver example, the nonlinear solution does not preserve the symmetry properties of the linearized model.

Finally, Figure 12 corresponds to a transfer maneuver in the transition zone, with $\chi = 1.6017\times 10^{1}$ and dimensionless thrust acceleration 3.2684×10^{-2}. Resulting times of flight are 9.1327 for

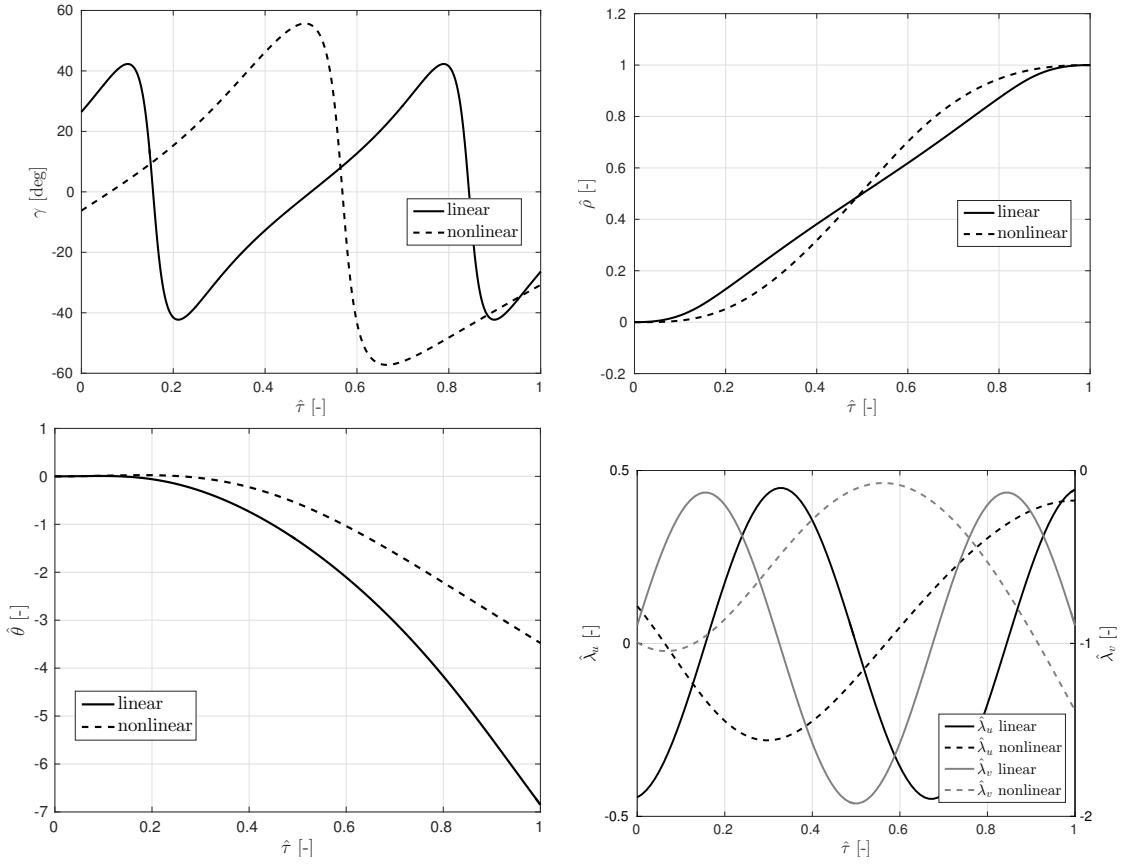

Fig. 12 Earth to Mars transfer for a non-dimensional thrust acceleration of 3.2684×10^{-2} (corresponding to $\chi = 1.6017\times10^{1}$).

the linearized maneuver and 6.9437 for the complete equations (corresponding to 1.4535 and 1.1051 revolutions of the reference orbit, respectively). The γ profile reflects the transition between both limit cases, showing an approximately one-period oscillation with large amplitude and characteristic features about the middle point of the maneuver. The radial distance profile is still similar to the short-maneuver case, but its secular behavior is transitioning from quadratic lo linear. The curves for $\hat{\lambda}_u$ and $\hat{\lambda}_v$ also present clear differences from the short-maneuver regime, beginning to develop the oscillatory behavior which characterizes the long-maneuver regime. Interestingly, the features observed for the linearized solution are more similar to the ones of the long-maneuver limit case, indicating that the nonlinearities increase the size of the transition zone in χ.

V. Application Examples

A. GEO Disposal

As a first application example we can consider an end-of-life disposal of a geostationary satellite ($R = 42164.14\,\mathrm{km}$) using an optimal low-thrust control strategy. Using Figure 2 as a reference, let us suppose the spacecraft is moved by $\Delta R = 200\,\mathrm{km}$ above the GEO protected region and let us assume a total mass $m = 1000\,\mathrm{kg}$ with 3 different low-thrust propulsion systems having maximum thrust F of 10 mN, 35 mN and 100 mN, respectively.

The value of the dimensionless radial change, $\Delta r = \Delta R/R = 4.74\times10^{-3}$, corresponds to a virtually linear problem, as it appears clearly in Figure 2. The corresponding non-dimensional thrust acceleration $\varepsilon = FR^2/(\mu m)$ for the three cases results in 4.46×10^{-5}, 1.56×10^{-4} and 4.46×10^{-4}, respectively. In turns, the parameter $\chi = \Delta r/\varepsilon$ for the three cases yields 106.35, 30.39 and 10.63, respectively.

The first case falls well in the long-maneuver regime, which implies a virtually tangential thrusting strategy with duration $\Delta\tau \simeq \chi/2 = 53.17$ corresponding to $\chi/(4\pi) = 8.46$ orbits or 8.44 solar days.

The second case still belongs to the long-maneuver regime but is closer to the transition zone, which brings non-negligible oscillations (at the orbital frequency) of the optimal thrust direction with respect to the tangential direction. The maneuver duration can be best predicted with the refined long-maneuver approximation [Eqs. (34-36)] as $\Delta\tau \simeq \chi/2\bar{C} = 16.0$ corresponding to 2.55 orbits or 2.54 solar days. As the maneuver duration is far from being a multiple of the orbit period part of the thrust resources are spent to meet the boundary conditions, which results in a larger duration compared to a nearly tangential strategy as discussed in Section III B.

The third case lies within the transition zone, as shown in Figure 2. A good estimate for the duration of the maneuver can still be obtained with the refined long-maneuver approximation, yielding $\Delta\tau \simeq \chi/2\bar{C} = 5.32$ corresponding to 0.846 orbits or 0.844 solar days. Because the maneuver takes less than one orbital revolution to complete the optimal thrust orientation will strongly separate from the tangential direction.

B. Simplified Earth-Mars Transfer

Another relevant application example is an Earth-to-Mars low-thrust transfer. As a very crude, but still useful approximation one can model both Mars and Earth orbits as circular and coplanar, assume the spacecraft departs from the same circular orbit as the Earth and neglect mass variations due to propellant consumption. In this case let us first consider a fixed trip time of 3 years to get a cargo spacecraft of masses 2000, 5000 and 10000 kg to Mars as a support for a subsequent human exploration mission. Let us employ the results of this article, and in particular the ones shown in Fig. 9, to estimate the required thrust force (assumed constant) and control strategy. The value of the dimensionless radial change, taking Earth semimajor axis ($R = a_0$ =1 AU) as reference radius and the semimajor axis of Mars orbit as arrival radius ($R + \Delta R = a_f$ =1.524 AU), is Δr=0.524, which highlights that that this transfer problem is far from linear. It is therefore recommended to adopt an intermediate orbit reference radius $R' = \left[\sqrt{a_0 a_f}\left(\sqrt{a_0} + \sqrt{a_f}\right)/2\right]^{2/3} =$ 1.239 AU, to minimize the error associated to the nonlinearities as discussed in Section III E. The new dimensionless radius change becomes $\Delta r' = 0.524/1.239 = 0.423$.

Since the period of the reference orbit is 1.379 years the required dimensionless transfer time is 2.175 revolutions or $\Delta\tau = 4.35\,\pi$, which implies we are in the long-maneuver regime. Following Eq. (32) we obtain $\chi \approx 2\Delta\tau$ =27.33 leading to $\varepsilon = \Delta r'/\chi = 0.0155$ thus requiring a thrust $F = \mu\varepsilon m/R'^2$ of 120, 300 and 600 mN, respectively.

The exact solution provided by Fig. 9 is $\chi = 25.91$, requiring a thrust magnitude of 126, 315 and 630 mN, respectively.

If the required trip time is now reduced to two years (corresponding to 1.45 revolutions or $\Delta\tau = 2.9\,\pi$) the optimization problem falls in the transition regime. From Fig. 9, one has $\chi \approx 15.7$ finally resulting in a required thrust magnitude of 208, 519 and 1038 mN, respectively, with, expectedly, a strongly non-tangential optimum thrust vector. Here Edelbaum's solution would largely underestimated the required thrust (Fig. 9). On the other hand the refined long-maneuver approximation ([Eqs. (34-36)]) provides quite accurate results with an estimated $\chi \approx 15.55$ corresponding to 206, 514 and 1028 mN of required thrust magnitude.

C. Hayabusa-2

The $\sim 600\,\mathrm{kg}$ Hayabusa-2 spacecraft will arrive at the $\sim 1\,\mathrm{km}$ diameter asteroid 162173 Ryugu in July 2018. According to (nominal) mission operations, the spacecraft will hover above the asteroid surface in a similar way as the Hayabusa-1 mission did [20]. Nevertheless, it is interesting to look at the case of a hypothetical orbiter and the requirements to change its altitude in an optimum way using the nominal $\sim 28\,\mathrm{mN}$ ion engine of the Hayabusa-2 mission. For a preliminary analysis, let us neglect all perturbations, assume an initial circular orbit of $20\,\mathrm{km}$ radius and optimize a $1\,\mathrm{km}$ radius change maneuver. Because $\Delta r = 0.05$ the maneuver can be considered linear. Assuming an average density of $2.0\,\mathrm{g/cm^3}$ and a spherical shape for Ryugu one obtains $\mu \approx 560\,\mathrm{m^3 s^{-2}}$, which corresponds to a period of roughly 9 days. In turns $\varepsilon \approx 33.3$ and $\chi = 1.5\times10^{-3}$ which falls well in the short-maneuver regime. This indicates that the optimum thrust orientation is practically bang-bang along the radial direction and the expected maneuver time is $\Delta\tau \simeq 2\sqrt{\chi} = 7.7\times10^{-2}$, which corresponds to about 2.57 hours.

VI. Conclusions

The minimum-time constant-thrust acceleration transfer between two coplanar, circular orbits has been studied in great detail, using a relative motion formulation in curvilinear coordinates and the indirect method. Together with a previous paper on the same-orbit rephasing problem, this work completes the study on the minimum-time constant-thrust control between circular orbits in curvilinear coordinates. Results show that the time-optimal transfer undergoes fundamental qualitative changes with the required time of flight, being possible to identify two limit cases, a short-maneuver and a long-maneuver regime, separated by a transition zone. This structure is similar to the one found for the rephasing case. The short- and long-maneuver limit regimes correspond, respectively, to transfers requiring much less or more than one revolution of the reference orbit to complete, whereas transfers in the transition zone present times of flight of approximately one period of the reference orbit. The qualitative characteristics of each region have been studied in detail using analytical and numerical techniques, both for the linearized and complete equations of motion, and three representative examples have been presented to illustrate them. For transfers in the short-

maneuver regime the thrust orientation control law is nearly bang-bang along the radial direction, being initially oriented along the desired radial displacement and changing direction halfway through the maneuver. Conversely, in the long-maneuver regime the optimal thrust orientation oscillates with small amplitude about the transversal direction, oriented along it for positive radial displacements and opposite to it for negative radial displacements. It is important to highlight that the whole spectrum of maneuvers (in terms of number of revolutions) has been characterized using a unified formulation which naturally led to the identification of the three regions, without additional a priori hypothesis.

The ratio of the required radial displacement and the available thrust acceleration is identified as the main parameter of the problem and a clear relation between this parameter and the time of flight is observed for both regimes. An approximate analytical study of the first order optimality conditions for the linearized equations of motion leads to explicit expressions for the time of flight depending only on the displacement-thrust ratio, as well as other estimations and qualitative information about the evolution of state and costate. Particularly, a suboptimal analytical solution fulfilling all the linearized differential equations and constraints is reached for the long-maneuver regime. Compared to Edelbaum's method, this refined solution is more complex to evaluate but provides more detailed information on the evolution of time of flight, state and costate. For the complete equations of motion, nonlinear effects make the solution dependent on two parameters (the radial displacement and the displacement over thrust ratio). The effect of the nonlinearities depends mainly on the required radial displacement, and it is especially important in the transition zone and the long-maneuver regime. Related to this, the choice of the reference orbit has a key impact in the deviation between the times of flight for the linear and nonlinear representations of dynamics, especially in the long-maneuver regime. By choosing an adequate reference orbit between the initial and final ones, it is possible to close the gap and make both coincide.

These approximate analytical solutions can be very useful to construct the initial guesses required by iterative numerical solvers for both the direct and indirect methods. Particularly, all the test cases for the linearized equations of motion were successfully solved using their approximate analytical solution as initial guess. Furthermore, the linearized solution can be used as initial guess

for the complete problem in many practical cases, especially for the short-maneuver regime or when the required radial displacement is small.

VII. Acknowledgments

This work has been supported by the Spanish Ministry of Education, Culture and Sport through its Formación del Profesorado Universitario Program (reference number FPU13/05910), and by the Spanish Ministry of Economy and Competitiveness within the framework of the research project "Dynamical Analysis, Advanced Orbital Propagation, and Simulation of Complex Space Systems" (ESP2013-41634-P). The authors also want to thank the funding received from the European Union Seventh Framework Programme (FP7/2007-2013) under grant agreement N 607457 (LEOSWEEP).

References

[1] T. N. Edelbaum, "Propulsion Requirements for Controllable Satellites," *ARS Journal*, Vol. 31, No. 8, 1961, pp. 1079–1089. doi:10.2514/8.5723.

[2] R. Broucke, "Low-Thrust Trajectory Optimization in an Inverse Square Force Field," *AAS/AIAA Spaceflight Mechanics Meeting*, No. AAS 91-159, Houston, Texas, USA, February 11-13 1991, pp. 182–204.

[3] L. J. Wood, "Perturbation Guidance for Minimum Time Flight Paths of Spacecraft," *AIAA/AAS Astrodynamics Conference*, No. AAS 72-915, Palo Alto, CA, USA, September 11-12 1972, pp. 1–11.

[4] J. D. Thorne and C. D. Hall, "Approximate Initial Lagrange Costates for Continuous-Thrust Spacecraft," *Journal of Guidance, Control, and Dynamics*, Vol. 19, No. 2, 1996, pp. 283–288. doi:10.2514/3.21616.

[5] S. Alfano and J. D. Thorne, "Circle-to-Circle Constant-Thrust Orbit Raising," *Journal of the Astronautical Sciences*, Vol. 42, No. 1, 1994, pp. 35–45.

[6] L. Casalino, "Approximate Optimization of Low-Thrust Transfers Between Low-Eccentricity Close Orbits," *Journal of Guidance, Control, and Dynamics*, Vol. 37, No. 3, 2014, pp. 1003–1008. doi:10.2514/1.62046.

[7] J. L. Gonzalo and C. Bombardelli, "Optimal Continuous-Thrust Rephasing Maneuver in Circular Orbit," *Journal of Guidance, Control, and Dynamics*, Vol. 40, 2017, pp. 1155–1165. doi: 10.2514/1.G002305.

[8] C. Bombardelli, J. L. Gonzalo, and J. Roa, "Approximate Solutions of Non-Linear Circular Orbit Relative Motion in Curvilinear Coordinates," *Celestial Mechanics and Dynamical Astronomy*, Vol. 127, No. 1, 2017, pp. 49–66. doi:10.1007/s10569-016-9716-x.

[9] W. Clohessy and R. Wiltshire, "Terminal Guidance System for Satellite Rendezvous," *Journal of the Aerospace Sciences*, Vol. 27, No. 9, 1960, pp. 653–658. doi:10.2514/8.8704.

[10] C. Bombardelli, J. L. Gonzalo, and J. Roa, "Compact Solution of Circular Orbit Relative Motion in Curvilinear Coordinates," *Astrodynamics 2015* (Univelt, ed.), Vol. 156 of *Advances in the Astronautical Sciences*, Vail, CO, USA, AAS/AIAA, August 9-13 2015, pp. 925–935. ISSN:0065-3438.

[11] A. E. Bryson and Y.-C. Ho, *Applied Optimal Control. Optimization, Estimation and Control.* Taylor & Francis, 1975. ISBN:978-0-89116-228-5.

[12] L. S. Pontryagin, V. G. Boltyanski, R. S. Gamkrelidze, and E. F. Mishchenko, *The Mathematical Theory of Optimal Processes.* Interscience, 1962.

[13] D. F. Lawden, *Optimal Trajectories for Space Navigation.* Butterworths, 1963.

[14] J. E. Prussing, *Primer Vector Theory and Applications*, pp. 16–36. Cambridge Aerospace Series, Cambridge University Press, 2010, 10.1017/CBO9780511778025.003.

[15] M. Pontani, "Symmetry Properties of Optimal Relative Orbit Trajectories," *Mathematical Problems in Engineering*, Vol. 2015, 2015. doi:10.1155/2015/286525.

[16] J. L. Gonzalo and C. Bombardelli, "Optimal Low Thrust Orbit Correction In Curvilinear Coordinates," *Astrodynamics 2015* (Univelt, ed.), Vol. 156 of *Advances in the Astronautical Sciences*, Vail, CO, USA, AAS/AIAA, August 9-13 2015, pp. 1875–1892. ISSN:0065-3438.

[17] C. Zhang, F. Topputo, F. Bernelli-Zazzera, and Y.-S. Zhao, "Low-Thrust Minimum-Fuel Optimization in the Circular Restricted Three-Body Problem," *Journal of Guidance, Control, and Dynamics*, Vol. 38, No. 8, 2015, pp. 1501–1510. doi:10.2514/1.G001080.

[18] "NASA Planetary Fact Sheet," `https://nssdc.gsfc.nasa.gov/planetary/factsheet/`. Accessed: 9 December 2016.

[19] "NASA Asteroid Fact Sheet," `https://nssdc.gsfc.nasa.gov/planetary/factsheet/asteroidfact.html`. Accessed: 9 December 2016.

[20] Y. Tsuda, M. Yoshikawa, M. Abe, H. Minamino, and S. Nakazawa, "System design of the Hayabusa 2 - asteroid sample return mission to 1999 JU3," *Acta Astronautica*, Vol. 91, 2013, pp. 356–362. doi:10.1016/j.actaastro.2013.06.028.